

A novel L-shaped refinement chain cuts method for two-stage stochastic programs

Mike Hewitt^{1†}, Francesca Maggioni^{2†}, Andrea Spinelli^{2†}

¹Department of Information System and Supply Chain Management,
Quinlan School of Business, Loyola University, 16 E Pearson St,
Chicago, 60611, IL, United States.

²Department of Management, Information and Production Engineering,
University of Bergamo, Viale G. Marconi 5, Dalmine, 24044, Italy.

Contributing authors: mhewitt3@luc.edu; francesca.maggioni@unibg.it;
andrea.spinelli@unibg.it;

[†]These authors contributed equally to this work.

Abstract

This paper introduces the *L-shaped refinement chain cuts method*, a novel approach for solving two-stage stochastic programs. The proposed method integrates the refinement chain of scenarios within the classical L-shaped decomposition framework. In the proposed approach, the full scenario set is partitioned into subgroups at each level of the refinement chain, and one subproblem is solved for each subgroup rather than for each individual scenario as in the classical L-shaped method. The proposed framework generalizes both the classical multi-cut and single-cut L-shaped formulations. Theoretical convergence properties to the optimal solution of the original two-stage stochastic program are established for every refinement level. In addition, the relationships between consecutive refinement levels are characterized in terms of Benders cuts, leading to the development of an iterative refinement-based solution algorithm across consecutive levels of the refinement chain. The effectiveness of the proposed method is evaluated on a two-stage stochastic fixed-charge multicommodity network design problem under a mean-risk formulation. Computational experiments on benchmark instances demonstrate the promising performance of the proposed framework and highlight its applicability to large-scale risk-averse stochastic optimization problems.

Keywords: Two-stage stochastic programming, L-shaped decomposition, Refinement chain, Stochastic network design model, Conditional value-at-risk

MSC Classification: [90C06](#), [90C11](#), [90C15](#), [90C46](#)

1 Introduction

In classical optimization problems, input parameters are often assumed to be known with certainty. In practice, however, these parameters frequently involve some level of uncertainty, which can compromise the reliability of deterministic solutions. To address this issue, several optimization approaches have been devised within the operations research literature that explicitly account for uncertainty into the optimization models. Among these, *Stochastic Programming* (see, e.g., [6; 30]) has emerged as one of the most prominent methodologies.

In a stochastic program, decisions are made in different stages depending on when the values of the stochastic parameters are revealed. *First-stage decisions* are made before any uncertainty is realized, while *recourse decisions* are taken in later stages once the information of the uncertain parameters becomes available. In this setting, the non-anticipativity constraints ensure that first-stage decisions remain identical at all stages, regardless of the realization of the uncertain parameters.

Stochastic programming formulations have an increasingly broad range of applications, including transportation and logistics (see, e.g., [50; 55]), network design (see, e.g., [3; 4]), and bike-sharing systems (see, e.g., [16; 34]), to name a few examples. In these application domains, first-stage decisions typically involve strategic planning choices, while recourse actions are implemented to mitigate the potentially disruptive realization of uncertainty.

To represent the possible outcomes of the uncertain parameters, a finite set of scenarios is typically introduced [17]. Since recourse decisions are defined with respect to the scenarios, the computational complexity of the model increases significantly as the size of the scenario tree grows. To address this challenge, two main research streams have emerged in the stochastic programming literature: decomposition techniques and bounding strategies.

On the one hand, decomposition techniques have been developed to partition the stochastic problem into smaller and more manageable subproblems [49]. Within this stream, one of the most prominent methods is the *L-shaped method* [5; 57], which extends the Benders decomposition approach originally introduced in [2] to stochastic programming. The procedure consists of three main steps [20; 21]: *projection*, *dualization* and *relaxation*. First, the original stochastic problem is projected onto the subspace defined by the first-stage variables. The resulting projected formulation is then dualized, yielding a set of valid inequalities that express, in terms of the first-stage decisions, the feasibility conditions (the so-called *feasibility cuts*), depending on the extreme rays of the dual feasible region, and the projected costs conditions (the so-called *optimality cuts*), depending on the extreme points of the dual feasible region. In principle, an equivalent reformulation could be obtained by including all possible feasibility and optimality cuts, which correspond to the enumeration of all extreme rays and extreme points of the dual feasible region, respectively. Since such enumeration is computationally intractable, a relaxation strategy is adopted in which only a subset of feasibility and optimality cuts is considered at each iteration of the procedure. This leads to the construction of a *master problem* and a sequence of *single-scenario subproblems* that are solved iteratively to identify the violated cuts and include them into the master problem in next iterations [42]. Depending on the level of aggregation,

the L-shaped method admits either a *multi-cut* formulation, generating one optimality cut per scenario [5], or a *single-cut* formulation, in which a single aggregated optimality cut is added to the master problem [57]. Intermediate formulations have also been proposed in the literature, where cuts derived from single-scenario subproblems in the multi-cut scheme are aggregated over groups of scenarios of different cardinalities [56].

The original Benders decomposition algorithm was designed for solving mixed-integer linear programming problems. However, thanks to the development of effective Benders-based heuristics, such approach has been widely adopted to address other classes of optimization problems, including nonlinear, integer, and bilevel formulations [42]. When applied to large-scale problems, particularly in the stochastic setting, a straightforward application of the classical Benders decomposition may exhibit limited computational efficiency. The main drawbacks include time-consuming iterations, weak feasibility and optimality cuts, and potential computational instability, to name a few. To mitigate these issues, various enhancement and acceleration techniques have been proposed. According to [42], four main directions can be identified in this setting: (i)-(ii) cut generation and solution generation approaches, aimed at reducing the number of iterations and producing high-quality cuts and solutions (see, e.g., [25; 28; 53]); (iii) solution procedures, referring to the algorithms used to solve the master problem and the subproblems, with the goal of improving convergence speed and reducing computational time per iteration (see, e.g., [44]); (iv) decomposition strategies which focus on how the problem is partitioned to obtain the initial master problem and the subproblems (see, e.g., [13]). However, it is worth noting that most of these improvements and developments have been proposed for the classical Benders decomposition, whereas relatively few studies have specifically focused on the L-shaped method (see, e.g., [1; 13; 31]), thereby motivating further research in this direction.

For very large-scale stochastic programs, obtaining an optimal solution within reasonable time may be challenging, even when decomposition strategies are employed. For this reason, a variety of bounding techniques and approximation schemes have been investigated to provide fast lower bounds on the optimal objective value of stochastic programs. According to [41], three main classes of approaches can be identified: bounds based on candidate policies; bounds based on refinement of the information structure, and bounds based on decision rules and aggregation. Since the approach adopted in this work belongs to the second class, we review the main contributions in the literature related to this line of research.

Refinement of the information structure involves splitting the scenario tree into smaller subtrees and optimizing decisions over these reduced structure. This leads to a collection of simpler optimization problems whose optimal values can be combined to yield a lower bound on the optimal value of the original stochastic problem. The most basic example of an information-structure refinement bound is the *Wait and See* (WS, see [6]), in which non-anticipativity constraints are relaxed and independent single-scenario subproblems are solved. Subproblems can be also defined over larger subsets of scenarios, consisting either of disjoint subgroups or of subgroups sharing reference scenarios that are fixed across all subsets [32; 33].

A broader framework based on refinement chains is introduced in [38], where monotonic chains of lower bounds are proposed for multistage stochastic programs with

concave risk functionals. In this setting, each bound is obtained by solving a collection of group subproblems that are less complex than the original problem, while appropriately recalculating the probabilities associated with the scenarios within each group. This refinement-based approach has been applied in [7] to address multistage distributionally robust optimization problems, and more recently in [40] to study two-stage stochastic programs under decision-dependent uncertainty. Alternative approaches for bounding risk-averse multistage stochastic programs rely on barycentric discretizations [19; 29], often combined with bounds based on first-order and convex-order stochastic dominance [39].

The idea of partitioning the scenario tree and applying scenario aggregation techniques has been widely explored in the stochastic programming literature, both for solving two-stage stochastic programs directly and within the context of the L-shaped decomposition method.

Several contributions investigate scenario aggregation without explicitly relying on the L-shaped method. In [54], an *Adaptive Partition Method* (APM) based on scenario aggregation is proposed to solve two-stage stochastic programs with discrete probability distributions. Sufficient and necessary conditions are derived to guarantee the existence of a completely sufficient partition, under which solving the stochastic program over the partition yields the same optimal solution as solving it over the original scenario tree. A *Generalized* version of APM, referred to as GAPM, is introduced in [47], where scenarios are initially fully aggregated and then iteratively disaggregated into subsets. An extension of the aggregation framework to settings with continuous distributions is developed. Scenario aggregation through clustering techniques is studied in [23], where clusters of scenarios are constructed and represented by selected representative scenarios to obtain smaller approximations of the original two-stage stochastic program. A generalization of the APM framework for solving chance-constrained stochastic programs with finite support has been recently discussed in [45].

Related lines of research embed scenario aggregation and partitioning techniques directly within the L-shaped decomposition framework, with the goal of strengthening the master problem and alleviating some of its computational drawbacks. In [56], an adaptive multi-cut method is proposed that generalizes both the single-cut and multi-cut L-shaped methods by dynamically adjusting the aggregation level of optimality cuts in the master problem. A related direction is pursued in [13], where a *Partial Benders Decomposition* (PBD) methodology is introduced, building on scenario retention and scenario creation strategies. The former projects the original two-stage stochastic program onto a larger subspace by relaxing only part of the problem, thereby reducing the number of feasibility cuts, while the latter aims at strengthening optimality cuts by generating artificial scenario subproblems and incorporating them into the master problem. The integration of GAPM with the L-shaped decomposition method is studied in [46], where sufficient conditions are provided to ensure that feasibility and optimality cuts constructed with respect to a scenario partition lead to an optimal solution. Applications of PBD to large-scale problems are presented in [27], addressing supply chain network design under uncertainty and enhancing PBD through tailored scenario creation strategies based on weighted estimators of expected values. More

recently, in [58] scenarios are clustered using neural networks and machine learning techniques, aggregating the corresponding Benders cuts within each cluster to solve stochastic facility location and production planning problems. Scenario aggregation techniques related to those in [13] have also been applied in [10] to address time-window assignment traveling salesperson problems with stochastic travel times.

1.1 Contributions

In this paper, we introduce a novel L-shaped refinement chain cuts method that integrates the refinement chain of scenarios proposed in [38] with the classical L-shaped decomposition method to solve two-stage stochastic programs. The main contributions of the paper are threefold and can be summarized as follows.

First, we develop a novel L-shaped method for each level of the refinement chain. While the classical L-shaped method solves one subproblem per scenario, our approach solves one subproblem per subgroup of scenarios. This results in fewer subproblems, each associated with scenario subgroups of larger cardinality. As in the classical L-shaped method, a single master problem is constructed for each level of the refinement chain, where optimality cuts are now specific for each subgroup. We prove that both the multi-cut and single-cut versions of the L-shaped method are special cases of our framework. Additionally, we provide a theoretical proof that, at each level of the refinement chain, the proposed method converges to the optimal solution of the original two-stage stochastic program.

Second, we investigate the relationship between consecutive levels of the refinement chain within the proposed L-shaped framework. In particular, we characterize how the dual feasible regions at two consecutive levels of the refinement chain are related, and how this relationship is reflected in the corresponding sets of extreme points. We show that the feasibility cuts of the classical L-shaped method remain valid at all refinement levels, whereas optimality cuts at a given level can be constructed as convex combinations of optimality cuts from the previous level using appropriately weights. This result enables the design of an iterative algorithm that solves the master problem at a given level of the refinement chain while incorporating optimality cuts obtained at the previous level.

Third, we evaluate the effectiveness of our method on a two-stage stochastic fixed-charge multicommodity network design problem, which commonly arises in various applications, particularly supply chain management and transportation. Stochastic optimization techniques have been mainly applied to network design problems by considering the minimization of expected value of the random parameters [13]. However, the use of alternative risk measures in this context remains relatively underexplored. For this reason, to address more general decision-making settings, we adopt a mean-risk formulation in which the objective function depends on both the expectation and the *Conditional Value-at-Risk* [52]. To the best of our knowledge, the present work and [15] represent the only contributions in the literature in which a mean-risk objective has been considered for a stochastic network design problem.

With respect to the existing literature on scenario aggregation and partitioning within L-shaped decomposition, the works most closely related to ours are [56] and [46]. Compared to [56], several key differences arise. First, our method allows subproblems

to be solved over groups of scenarios at a given level of the refinement chain, rather than requiring the solution of single-scenario subproblems. Second, we consider a more general setting for constructing the refinement chain of the scenario tree, going beyond disjoint scenario partitions. Third, we explicitly characterize the relationships between extreme points, optimality cuts, and feasibility cuts across consecutive levels of the refinement chain. With respect to [46], our approach preserves convergence without imposing additional conditions on the structure of the dual subproblems and allows the second-stage cost to be uncertain. Therefore, the proposed method provides a more general and flexible refinement-based integration of scenario aggregation within the L-shaped framework.

Overall, the research presented in this work contributes to the advancement of the stochastic programming literature by introducing a novel L-shaped refinement chain cuts method that integrates scenario partition within a decomposition framework. The proposed approach enhances methodological flexibility by enabling the solution of aggregated subproblems while preserving convergence guarantees and exploiting theoretical relationships across refinement levels. In addition, the incorporation of a mean-risk objective extends the applicability of the method to risk-averse decision-making settings.

The remainder of the paper is organized as follows. Section 2 presents the problem formulation and reviews the classical L-shaped decomposition method [5; 57]. Section 3 discusses the refinement chain of probabilities introduced in [38]. Section 4 integrates the refinement chain of probabilities into the L-shaped decomposition method, first at a fixed refinement level and then by analyzing the relationships between consecutive levels. Section 5 presents the implementation framework together with an iterative algorithm based on the proposed L-shaped refinement chain cuts method. Section 6 introduces the two-stage stochastic fixed-charge multicommodity network design problem and discusses the results of the computational experiments. Finally, Section 7 summarizes the main findings and outlines directions for future research.

2 L-shaped decomposition for two-stage stochastic programs

In this section, we briefly review the formulation of a two-stage stochastic program and the structure of the classical L-shaped decomposition method designed to solve it.

Let \mathbb{R}^n and $\mathbb{R}^{m \times n}$ denote the space of n -dimensional real vectors and $m \times n$ real matrices, respectively. Let $\mathbf{x} \in \mathcal{X} \subseteq \mathbb{R}^n$ represent first-stage decision variables, with \mathcal{X} a non-empty closed set. We consider a stochastic parameter $\boldsymbol{\xi}$ defined on a probability space $(\Omega, \mathcal{A}, \mathbb{P})$. If $\boldsymbol{\xi}$ evolves as a discrete-time stochastic process over the finite support Ω , the information structure can be described in the form of a scenario tree. Let $\mathcal{S} := \{\boldsymbol{\omega}^1, \dots, \boldsymbol{\omega}^{|\mathcal{S}|}\}$ be the set of possible scenarios $\boldsymbol{\omega}^s \in \Omega$, each occurring with probability $p^s := \mathbb{P}(\boldsymbol{\omega}^s)$. With a slight abuse of notation, in the following we use s and $\boldsymbol{\omega}^s$ interchangeably to denote the s -th scenario. For each scenario $s \in \mathcal{S}$, let $\mathbf{y}^s \in \mathbb{R}^m$ denote the second-stage decision variables, constrained to satisfy the conditions $\mathbf{W}\mathbf{y}^s + \mathbf{T}^s\mathbf{x} = \mathbf{h}^s$ and $\mathbf{y}^s \geq \mathbf{0}$. We assume a fixed recourse matrix $\mathbf{W} \in \mathbb{R}^{p \times m}$, while the technology matrix $\mathbf{T}^s \in \mathbb{R}^{p \times n}$ and the right-hand side vector $\mathbf{h}^s \in \mathbb{R}^p$ depend

on scenario $s \in \mathcal{S}$. We associate fixed objective function coefficients $\mathbf{c} \in \mathbb{R}^n$ with the first-stage variables and scenario-dependent costs $\mathbf{q}^s \in \mathbb{R}^m$, $s \in \mathcal{S}$ with the second-stage variables. Finally, let $\boldsymbol{\xi}^s := (\mathbf{T}^s, \mathbf{h}^s, \mathbf{q}^s)$ denote the realization of the stochastic parameter $\boldsymbol{\xi}$ under scenario $s \in \mathcal{S}$.

The corresponding two-stage stochastic program can be therefore expressed as follows (see, e.g., [6]):

$$\min_{\mathbf{x}} \quad \mathbf{c}^\top \mathbf{x} + \sum_{s \in \mathcal{S}} p^s \mathcal{Q}(\mathbf{x}, \boldsymbol{\xi}^s) \quad (1a)$$

$$\text{s.t.} \quad \mathbf{x} \in \mathcal{X}, \quad (1b)$$

where, for each $s \in \mathcal{S}$, $\mathcal{Q}(\mathbf{x}, \boldsymbol{\xi}^s)$ is the *recourse* (or *second-stage*) *problem* associated with the realization $\boldsymbol{\xi}^s$, defined as follows:

$$\mathcal{Q}(\mathbf{x}, \boldsymbol{\xi}^s) := \min_{\mathbf{y}^s} \quad \mathbf{q}^{s\top} \mathbf{y}^s \quad (2a)$$

$$\text{s.t.} \quad \mathbf{W} \mathbf{y}^s = \mathbf{h}^s - \mathbf{T}^s \mathbf{x} \quad (2b)$$

$$\mathbf{y}^s \geq \mathbf{0}. \quad (2c)$$

Extensively, the *deterministic equivalent* of Problem (1) can be formulated as:

$$\min_{\mathbf{x}, \mathbf{y}^s} \quad \mathbf{c}^\top \mathbf{x} + \sum_{s \in \mathcal{S}} p^s \mathbf{q}^{s\top} \mathbf{y}^s \quad (3a)$$

$$\text{s.t.} \quad \mathbf{W} \mathbf{y}^s = \mathbf{h}^s - \mathbf{T}^s \mathbf{x} \quad \forall s \in \mathcal{S} \quad (3b)$$

$$\mathbf{y}^s \geq \mathbf{0} \quad \forall s \in \mathcal{S} \quad (3c)$$

$$\mathbf{x} \in \mathcal{X}. \quad (3d)$$

Note that the optimization in the second-stage is performed with respect to the expected value $\mathbb{E}_{\mathbb{P}}[\mathcal{Q}(\mathbf{x}, \boldsymbol{\xi})] := \sum_{s \in \mathcal{S}} p^s \mathbf{q}^{s\top} \mathbf{y}^s$. However, in a more general setting, this term can be replaced by a coherent risk measure $\varrho_{\mathbb{P}}[\mathcal{Q}(\mathbf{x}, \boldsymbol{\xi})]$ admitting a linear decomposition, such as the *Conditional Value-at-Risk* (CVaR) or the *mean-semideviation* risk measure (see, e.g., [18]). Such extensions are explored in the numerical experiments.

In what follows, we outline the L-shaped decomposition method proposed in [5; 57] to solve Problem (1). We begin by rewriting such problem as:

$$\min_{\mathbf{x}, \theta^s} \quad \mathbf{c}^\top \mathbf{x} + \sum_{s \in \mathcal{S}} p^s \theta^s \quad (4a)$$

$$\text{s.t.} \quad \mathcal{Q}(\mathbf{x}, \boldsymbol{\xi}^s) \leq \theta^s \quad \forall s \in \mathcal{S} \quad (4b)$$

$$\theta^s \in \mathbb{R} \quad \forall s \in \mathcal{S} \quad (4c)$$

$$\mathbf{x} \in \mathcal{X}, \quad (4d)$$

where, for each $s \in \mathcal{S}$, θ^s is an epigraph variable of the recourse problem $\mathcal{Q}(\mathbf{x}, \boldsymbol{\xi}^s)$.

If first-stage variables $\mathbf{x} \in \mathcal{X}$ are fixed and the realization $\boldsymbol{\xi}^s$ is observed, the right-hand side of (2b) becomes known. Thus, scenario subproblem (2) can be dualized by means of dual variables $\boldsymbol{\lambda} \in \mathbb{R}^p$, yielding to:

$$\mathcal{Q}_{dual}(\mathbf{x}, \boldsymbol{\xi}^s) := \max_{\boldsymbol{\lambda}} (\mathbf{h}^s - \mathbf{T}^s \mathbf{x})^\top \boldsymbol{\lambda} \quad (5a)$$

$$\text{s.t. } \mathbf{W}^\top \boldsymbol{\lambda} \leq \mathbf{q}^s. \quad (5b)$$

If the dual feasible region $\Lambda^s := \{\boldsymbol{\lambda} \in \mathbb{R}^p : \mathbf{W}^\top \boldsymbol{\lambda} \leq \mathbf{q}^s\}$, defined by (5b), is not empty, as in relatively complete recourse case [6], Problem (5) can be either unbounded or feasible for any possible choice of \mathbf{x} [42].

Based on duality theory, in the case of unboundedness of the dual problem (5), its corresponding primal problem (2) is infeasible. Therefore, if $\mathcal{R}(\Lambda^s)$ is the set of extreme rays of Λ^s , there exists a direction $\mathbf{r} \in \mathcal{R}(\Lambda^s)$ for which $(\mathbf{h}^s - \mathbf{T}^s \mathbf{x})^\top \mathbf{r} > 0$. To avoid this situation and prevent movements in any potential direction of unboundedness, the following *feasibility cut* is imposed in Problem (4):

$$(\mathbf{h}^s - \mathbf{T}^s \mathbf{x})^\top \mathbf{r} \leq 0 \quad \forall \mathbf{r} \in \mathcal{R}(\Lambda^s), \forall s \in \mathcal{S}. \quad (6)$$

On the other hand, in the case of feasibility of Problem (5), its optimal solution is one of the extreme points $\mathbf{e} \in \mathcal{E}(\Lambda^s)$ of the dual feasible region, being $\mathcal{E}(\Lambda^s)$ the set of extreme points of Λ^s . Thus, to bound the optimal value of Problem (5), and hence of Problem (2) by strong duality, the following *optimality cut* is added to Problem (4):

$$(\mathbf{h}^s - \mathbf{T}^s \mathbf{x})^\top \mathbf{e} \leq \theta^s \quad \forall \mathbf{e} \in \mathcal{E}(\Lambda^s), \forall s \in \mathcal{S}. \quad (7)$$

Consequently, Problem (4) can be reformulated as follows:

$$\min_{\mathbf{x}, \theta^s} \mathbf{c}^\top \mathbf{x} + \sum_{s \in \mathcal{S}} p^s \theta^s \quad (8a)$$

$$\text{s.t. } (\mathbf{h}^s - \mathbf{T}^s \mathbf{x})^\top \mathbf{r} \leq 0 \quad \forall \mathbf{r} \in \mathcal{R}(\Lambda^s), \forall s \in \mathcal{S} \quad (8b)$$

$$(\mathbf{h}^s - \mathbf{T}^s \mathbf{x})^\top \mathbf{e} \leq \theta^s \quad \forall \mathbf{e} \in \mathcal{E}(\Lambda^s), \forall s \in \mathcal{S} \quad (8c)$$

$$\theta^s \in \mathbb{R} \quad \forall s \in \mathcal{S} \quad (8d)$$

$$\mathbf{x} \in \mathcal{X}. \quad (8e)$$

We will refer to Problem (8) as the *Benders master problem*.

Note that solving Problem (8) requires enumerating all the extreme points $\mathbf{e} \in \mathcal{E}(\Lambda^s)$ and all the extreme rays $\mathbf{r} \in \mathcal{R}(\Lambda^s)$ for all $s \in \mathcal{S}$, which is generally not practical. To address this issue, the L-shaped method relaxes Problem (8) and solves it iteratively, considering only a subset of constraints (8b) and (8c) and yielding a trial solution $\bar{\mathbf{x}} \in \mathcal{X}$ at each iteration. The dual subproblem (5) is then solved with $\mathbf{x} = \bar{\mathbf{x}}$ in (5a) for each scenario $s \in \mathcal{S}$ with the aim of identifying any possibly violated optimality and feasibility cuts. When these violated cuts are determined, they are added to the relaxation of the master problem and the process is repeated. Note that the procedure converges in a finite number of steps since both $|\mathcal{E}(\Lambda^s)|$ and $|\mathcal{R}(\Lambda^s)|$ are

finite, for all $s \in \mathcal{S}$. This solution process is often referred to as the *multi-cut* version of the L-shaped method, as one cut is constructed for each scenario [5]. Conversely, it is possible to aggregate all second-stage epigraph variables θ^s into a single variable $\Theta \in \mathbb{R}$, leading to the following *single-cut* reformulation of the master problem [57]:

$$\min_{\mathbf{x}, \Theta} \quad \mathbf{c}^\top \mathbf{x} + \Theta \quad (9a)$$

$$\text{s.t.} \quad (\mathbf{h}^s - \mathbf{T}^s \mathbf{x})^\top \mathbf{r} \leq 0 \quad \forall \mathbf{r} \in \mathcal{R}(\Lambda^s), \forall s \in \mathcal{S} \quad (9b)$$

$$\sum_{s \in \mathcal{S}} p^s (\mathbf{h}^s - \mathbf{T}^s \mathbf{x})^\top \mathbf{e}^s \leq \Theta \quad \forall \mathbf{e}^s \in \mathcal{E}(\Lambda^s), \forall s \in \mathcal{S} \quad (9c)$$

$$\Theta \in \mathbb{R} \quad (9d)$$

$$\mathbf{x} \in \mathcal{X}. \quad (9e)$$

Note that the optimality cut (9c) can be included in the master problem only when the trial first-stage solution $\bar{\mathbf{x}}$ yields feasible subproblems $\mathcal{Q}(\bar{\mathbf{x}}, \boldsymbol{\xi}^s)$ for all scenarios $s \in \mathcal{S}$. If this condition is not satisfied, only the feasibility cuts (9b) are added, until a first-stage solution that ensures feasibility across all subproblems is found, allowing the generation of the optimality cut (9c).

When comparing the multi-cut and single-cut formulations, the main differences lie in how much dual information each approach retains and correspondingly in the resulting size of the Benders master problem [56]. The single-cut version aggregates the dual information from all scenarios into a single optimality cut, which results in a weaker informative power. In contrast, the multi-cut method preserves the full dual information by generating one cut per scenario, often resulting in faster convergence in terms of number of iterations. However, as the number of scenarios increases, the master problem in the multi-cut formulation grows significantly because of the large number of cuts [46].

3 Refinement chain of probabilities

In this section, we review the refinement chain framework and the associated probability dissection proposed in [38].

Assume that the support Ω of the uncertain parameter $\boldsymbol{\xi}$ can be decomposed into finite sequences of subsets, forming a *refinement chain* with J levels. Each level $j = 1, \dots, J$ of the refinement chain is a collection $\{\Omega_i^{(j)}\}_{i=1}^{m_j}$ of m_j subsets containing scenarios sampled from \mathcal{S} , as follows:

$$\begin{array}{ll} \text{level } J & \Omega_1^{(J)} = \Omega \\ & \vdots \\ \text{level } j & (\Omega_1^{(j)}, \Omega_2^{(j)}, \dots, \Omega_{m_j}^{(j)}) \\ & \vdots \\ \text{level } 1 & (\Omega_1^{(1)}, \Omega_2^{(1)}, \dots, \Omega_{m_1}^{(1)}). \end{array} \quad (10)$$

In the construction of the refinement chain (10) two properties must hold:

(R1) at each level $j = 1, \dots, J$, the union of subsets $\{\Omega_i^{(j)}\}_{i=1}^{m_j}$ covers the whole support, i.e.:

$$\Omega = \bigcup_{i=1}^{m_j} \Omega_i^{(j)} \quad \forall j = 1, \dots, J;$$

(R2) each set $\Omega_i^{(j)}$ at level $j = 2, \dots, J$ is the union of sets $\{\Omega_{k_1}^{(j-1)}, \dots, \Omega_{k_{N_i}}^{(j-1)}\}$ from the next more refined collection at level $j - 1$, i.e.:

$$\Omega_i^{(j)} = \bigcup_{\ell=1}^{N_i} \Omega_{k_\ell}^{(j-1)} \quad \forall j = 2, \dots, J, \forall i = 1, \dots, m_j.$$

The refinement chain (10) of Ω is associated with a corresponding chain of dissections of the probability measure \mathbb{P} defined as follows:

$$\begin{array}{rcl} \text{level } J & \mathbb{P}_1^{(J)} = \mathbb{P} & \\ \vdots & \vdots & \\ \text{level } j & (\mathbb{P}_1^{(j)}, \mathbb{P}_2^{(j)}, \dots, \mathbb{P}_{m_j}^{(j)}) & (11) \\ \vdots & \vdots & \\ \text{level } 1 & (\mathbb{P}_1^{(1)}, \mathbb{P}_2^{(1)}, \dots, \mathbb{P}_{m_1}^{(1)}). & \end{array}$$

The following properties on the chain of probabilities must be satisfied:

- (P1) each probability measure $\mathbb{P}_i^{(j)}$ has support $\Omega_i^{(j)}$, $\forall j = 1, \dots, J$, $\forall i = 1, \dots, m_j$;
(P2) at each level $j = 1, \dots, J$, the probability measure \mathbb{P} can be decomposed into a convex combination of probabilities $\{\mathbb{P}_i^{(j)}\}_{i=1}^{m_j}$ with weights $\pi_i^{(j)}$, i.e.:

$$\mathbb{P} = \sum_{i=1}^{m_j} \pi_i^{(j)} \mathbb{P}_i^{(j)} \quad (12)$$

where $\pi_i^{(j)} \geq 0 \forall i = 1, \dots, m_j$ and $\sum_{i=1}^{m_j} \pi_i^{(j)} = 1$, $\forall j = 1, \dots, J$;

- (P3) for each level $j = 2, \dots, J$ and for each $i = 1, \dots, m_j$, the probability measure $\mathbb{P}_i^{(j)}$ can be decomposed into a convex combination of probability measures $\{\mathbb{P}_{k_1}^{(j-1)}, \dots, \mathbb{P}_{k_{N_i}}^{(j-1)}\}$ from the refined collection at level $j - 1$ with weights $\{\pi_{k_1, i}^{(j-1, j)}, \dots, \pi_{k_{N_i}, i}^{(j-1, j)}\}$, i.e.:

$$\mathbb{P}_i^{(j)} = \sum_{\ell=1}^{N_i} \pi_{k_\ell, i}^{(j-1, j)} \mathbb{P}_{k_\ell}^{(j-1)} \quad (13)$$

with $\pi_{k_\ell, i}^{(j-1, j)} \geq 0 \forall \ell = 1, \dots, N_i$ and $\sum_{\ell=1}^{N_i} \pi_{k_\ell, i}^{(j-1, j)} = 1$, $\forall j = 2, \dots, J$.

Within the notation introduced so far, we will refer to $\pi_i^{(j)}$ and $\pi_{k_\ell, i}^{(j-1, j)}$ as *intra-level* and *inter-level* weights, respectively.

A refinement chain can be constructed in multiple ways, provided that properties (R1)–(R2) and (P1)–(P3) are satisfied. However, two natural approaches can be considered: (i) keeping one or more scenarios fixed across subsets, so they appear in all subsets at all levels; (ii) forming disjoint partitions at each level. In the following, we examine these two cases further.

Fixed scenarios

Assume that at level $j \in \{1, \dots, J\}$, the first $f \geq 1$ scenarios are fixed and included in all subset $\Omega_i^{(j)}$, $\forall i = 1, \dots, m_j$. Consequently, the probability measure $\mathbb{P}_i^{(j)}$ supported on $\Omega_i^{(j)}$ can be represented as the sum of Dirac measures δ_{ω^s} over the first f scenarios and the remaining ones, as follows:

$$\mathbb{P}_i^{(j)} = \sum_{s=1}^f p^s \delta_{\omega^s} + \sum_{s=f+1}^{|\Omega_i^{(j)}|} \frac{1 - \sum_{k=1}^f p^k}{\sum_{k=f+1}^{|\Omega_i^{(j)}|} p^k} p^s \delta_{\omega^s},$$

where $|\Omega_i^{(j)}|$ represents the number of scenarios in $\Omega_i^{(j)}$. Thus, by defining $p_{\Omega_i^{(j)}}^s := \mathbb{P}_i^{(j)}(\omega^s)$ as the probability of scenario ω^s as an element of subset $\Omega_i^{(j)}$, we have that:

$$p_{\Omega_i^{(j)}}^s = \begin{cases} p^s & \forall s = 1, \dots, f \\ \frac{1 - \sum_{k=1}^f p^k}{\sum_{k=f+1}^{|\Omega_i^{(j)}|} p^k} p^s & \forall s = f + 1, \dots, |\Omega_i^{(j)}|. \end{cases} \quad (14)$$

The intra-level weights $\pi_i^{(j)}$ in the convex combination (12) are calculated as follows:

$$\pi_i^{(j)} = \frac{\sum_{k=f+1}^{|\Omega_i^{(j)}|} p^k}{1 - \sum_{k=1}^f p^k}. \quad (15)$$

Disjoint partitions

Suppose that at level $j \in \{1, \dots, J\}$ all subsets $\Omega_i^{(j)}$ are disjoint. In this case, the probability measure $\mathbb{P}_i^{(j)}$ equals to:

$$\mathbb{P}_i^{(j)} = \sum_{s: \omega^s \in \Omega_i^{(j)}} \frac{p^s}{\sum_{k: \omega^k \in \Omega_i^{(j)}} p^k} \delta_{\omega^s},$$

and accordingly the probability $p_{\Omega_i^{(j)}}^s$ is:

$$p_{\Omega_i^{(j)}}^s = \frac{p^s}{\sum_{k: \omega^k \in \Omega_i^{(j)}} p^k}. \quad (16)$$

For disjoint partitions, the intra-level weights $\pi_i^{(j)}$ are as follows:

$$\pi_i^{(j)} = \sum_{k:\omega^k \in \Omega_i^{(j)}} p^k. \quad (17)$$

The following remarks hold for the two considered approaches (fixed scenarios and disjoint partitions), when examining two consecutive levels j and $j-1$ of the refinement chain, with $j \in \{2, \dots, J\}$.

Remark 1 There exists a closed-form expression for the inter-level weights $\pi_{k_\ell, i}^{(j-1, j)}$ given the intra-level weights $\pi_{k_\ell}^{(j-1)}$ and $\pi_i^{(j)}$, as follows:

$$\pi_{k_\ell, i}^{(j-1, j)} = \frac{\pi_{k_\ell}^{(j-1)}}{\pi_i^{(j)}} \quad \forall \ell = 1, \dots, N_i, \forall j = 2, \dots, J. \quad (18)$$

Remark 2 It is possible to characterize the intra-level weights between two consecutive levels, as stated in the following lemma.

Lemma 1 According to property (R2), suppose that $\Omega_i^{(j)} = \bigcup_{\ell=1}^{N_i} \Omega_{k_\ell}^{(j-1)}$, with $j \in \{2, \dots, J\}$ and $i \in \{1, \dots, m_j\}$. Then:

$$\pi_i^{(j)} = \sum_{\ell=1}^{N_i} \pi_{k_\ell}^{(j-1)}. \quad (19)$$

Proof We discuss the two cases separately.

On the one hand, if all subsets $\Omega_{k_\ell}^{(j-1)}$ have the first $f \geq 1$ scenarios fixed, then, according to (15), we have that:

$$\begin{aligned} \sum_{\ell=1}^{N_i} \pi_{k_\ell}^{(j-1)} &= \sum_{\ell=1}^{N_i} \frac{\sum_{s=f+1}^{|\Omega_{k_\ell}^{(j-1)}|} p^s}{1 - \sum_{s=1}^f p^s} \\ &= \frac{1}{1 - \sum_{s=1}^f p^s} \sum_{\ell=1}^{N_i} \sum_{s=f+1}^{|\Omega_{k_\ell}^{(j-1)}|} p^s \\ &= \frac{1}{1 - \sum_{s=1}^f p^s} \sum_{s=f+1}^{|\Omega_i^{(j-1)}|} p^s \\ &= \pi_i^{(j)}, \end{aligned}$$

where, in the third equality, we use the fact that each non-fixed scenario belongs to exactly one subset $\Omega_{k_\ell}^{(j-1)}$.

On the other hand, if all subsets $\Omega_{k_\ell}^{(j-1)}$ are disjoint, then, according to (17), it holds that:

$$\begin{aligned}
\pi_i^{(j)} &= \sum_{s: \omega^s \in \Omega_i^{(j)}} p^s \\
&= \sum_{s: \omega^s \in \bigcup_{\ell=1}^{N_i} \Omega_{k_\ell}^{(j-1)}} p^s \\
&= \sum_{s: \omega^s \in \Omega_{k_1}^{(j-1)}} p^s + \dots + \sum_{s: \omega^s \in \Omega_{k_{N_i}}^{(j-1)}} p^s \\
&= \pi_{k_1}^{(j-1)} + \dots + \pi_{k_{N_i}}^{(j-1)} \\
&= \sum_{\ell=1}^{N_i} \pi_{k_\ell}^{(j-1)},
\end{aligned}$$

where, in the third equality, similarly as before, we rely on the fact that each scenario in $\Omega_i^{(j)}$ belongs to exactly one subset $\Omega_{k_\ell}^{(j-1)}$. \square

The construction of the refinement chain reviewed so far, together with the results on the L-shaped method discussed in Section 2, provides the theoretical foundation required for the developments presented in the following sections.

4 Integrating refinement chain into L-shaped decomposition method

In this section, we integrate the refinement chain of probabilities into the L-shaped decomposition method. We begin by describing our novel approach for a fixed level of the refinement chain (see Section 4.1). Then, we examine the relationship in terms of dual feasible regions and Benders cuts between consecutive levels of the refinement chain (see Section 4.2).

4.1 L-shaped method over a fixed level of the refinement chain

As described in Section 2, in the classical L-shaped decomposition method a sequence of $|\mathcal{S}|$ single-scenario subproblems (5) is iteratively solved to identify feasibility and optimality cuts (8b)–(8c). Suppose now that a refinement chain (10) is provided and consider a given level $j \in \{1, \dots, J\}$ composed by m_j subsets $\{\Omega_1^{(j)}, \dots, \Omega_{m_j}^{(j)}\}$. We begin by reformulating Problem (4) so that, in the second stage, scenarios are not treated individually but are instead grouped within these subsets.

For each $i = 1, \dots, m_j$, we introduce $\theta_i^{(j)}$ as an epigraph variable of the recourse function $\mathcal{Q}(\mathbf{x}, \boldsymbol{\xi}_i^{(j)})$ defined over subset $\Omega_i^{(j)}$ of scenarios, where $\boldsymbol{\xi}_i^{(j)} := (\mathbf{T}_i^{(j)}, \mathbf{h}_i^{(j)}, \mathbf{q}_i^{(j)})$ denotes the realization of the uncertain parameters within $\Omega_i^{(j)}$. The resulting *two-stage stochastic problem at level j* can thus be written as:

$$\min_{\mathbf{x}, \theta_i^{(j)}} \mathbf{c}^\top \mathbf{x} + \sum_{i=1}^{m_j} \pi_i^{(j)} \theta_i^{(j)} \tag{20a}$$

$$\text{s.t. } \mathcal{Q}(\mathbf{x}, \boldsymbol{\xi}_i^{(j)}) \leq \theta_i^{(j)} \quad \forall i = 1, \dots, m_j \quad (20b)$$

$$\theta_i^{(j)} \in \mathbb{R} \quad \forall i = 1, \dots, m_j \quad (20c)$$

$$\mathbf{x} \in \mathcal{X}, \quad (20d)$$

where the recourse problem $\mathcal{Q}(\mathbf{x}, \boldsymbol{\xi}_i^{(j)})$ is defined as:

$$\mathcal{Q}(\mathbf{x}, \boldsymbol{\xi}_i^{(j)}) := \min_{\mathbf{y}^s: \boldsymbol{\omega}^s \in \Omega_i^{(j)}} \sum_{s: \boldsymbol{\omega}^s \in \Omega_i^{(j)}} p_{\Omega_i^{(j)}}^s \mathbf{q}^{s\top} \mathbf{y}^s \quad (21a)$$

$$\text{s.t. } \mathbf{W} \mathbf{y}^s = \mathbf{h}^s - \mathbf{T}^s \mathbf{x} \quad \forall s: \boldsymbol{\omega}^s \in \Omega_i^{(j)} \quad (21b)$$

$$\mathbf{y}^s \geq \mathbf{0} \quad \forall s: \boldsymbol{\omega}^s \in \Omega_i^{(j)}. \quad (21c)$$

The weights $\pi_i^{(j)}$ in the objective function (20a) correspond to the intra-level weights introduced in Section 3.

For each scenario $\boldsymbol{\omega}^s \in \Omega_i^{(j)}$, we introduce a dual variable $\boldsymbol{\lambda}^s \in \mathbb{R}^p$ associated with constraint (21b). The dual problem of Problem (21) is then given by:

$$\mathcal{Q}_{dual}(\mathbf{x}, \boldsymbol{\xi}_i^{(j)}) := \max_{\boldsymbol{\lambda}^s: \boldsymbol{\omega}^s \in \Omega_i^{(j)}} \sum_{s: \boldsymbol{\omega}^s \in \Omega_i^{(j)}} (\mathbf{h}^s - \mathbf{T}^s \mathbf{x})^\top \boldsymbol{\lambda}^s \quad (22a)$$

$$\text{s.t. } \mathbf{W}^\top \boldsymbol{\lambda}^s \leq p_{\Omega_i^{(j)}}^s \mathbf{q}^s \quad \forall s: \boldsymbol{\omega}^s \in \Omega_i^{(j)}, \quad (22b)$$

where constraints (22b) define the dual feasible region $(\Lambda_i^{(j)})^s := \{\boldsymbol{\lambda}^s \in \mathbb{R}^p : \mathbf{W}^\top \boldsymbol{\lambda}^s \leq p_{\Omega_i^{(j)}}^s \mathbf{q}^s\}$ for each scenario $\boldsymbol{\omega}^s \in \Omega_i^{(j)}$. Considering the collection of all scenarios in $\Omega_i^{(j)}$, the dual feasible region $\Lambda_i^{(j)}$ of Problem (22) is then:

$$\Lambda_i^{(j)} := \bigtimes_{s: \boldsymbol{\omega}^s \in \Omega_i^{(j)}} (\Lambda_i^{(j)})^s \subseteq \mathbb{R}^{p \cdot |\Omega_i^{(j)}|}. \quad (23)$$

As in the classical L-shaped method, let $\mathcal{E}(\Lambda_i^{(j)})$ and $\mathcal{R}(\Lambda_i^{(j)})$ denote the sets of extreme points and extreme rays of $\Lambda_i^{(j)}$, respectively, for each $i = 1, \dots, m_j$. Based on this construction, we define the *Benders master problem at level j of the refinement chain* as:

$$\min_{\mathbf{x}, \theta_i^{(j)}} \mathbf{c}^\top \mathbf{x} + \sum_{i=1}^{m_j} \pi_i^{(j)} \theta_i^{(j)} \quad (24a)$$

$$\text{s.t. } (\mathbf{h}_i^{(j)} - \mathbf{T}_i^{(j)} \mathbf{x})^\top \mathbf{r} \leq 0 \quad \forall \mathbf{r} \in \mathcal{R}(\Lambda_i^{(j)}), \forall i = 1, \dots, m_j \quad (24b)$$

$$(\mathbf{h}_i^{(j)} - \mathbf{T}_i^{(j)} \mathbf{x})^\top \mathbf{e} \leq \theta_i^{(j)} \quad \forall \mathbf{e} \in \mathcal{E}(\Lambda_i^{(j)}), \forall i = 1, \dots, m_j \quad (24c)$$

$$\theta_i^{(j)} \in \mathbb{R} \quad \forall i = 1, \dots, m_j \quad (24d)$$

$$\mathbf{x} \in \mathcal{X}. \quad (24e)$$

Compared to the classical L-shaped formulation, the following observations can be made. First, the dual feasible region $\Lambda_i^{(j)}$ in (23) is not fixed, as it depends on the specific composition of scenarios in subset $\Omega_i^{(j)}$. Similarly, the dual feasible region Λ^s in (5b) varies across scenarios $s \in \mathcal{S}$. However, in Problem (24), only a sequence of m_j subproblems (22) is solved at each iteration, rather than $|\mathcal{S}|$ as in the classical L-shaped approach. Second, the multi-cut version of the L-shaped method [5] can be regarded as a special case of our approach, corresponding to the bottom level $j = 1$ of a refinement chain with disjoint subsets. Indeed, in this setting, $m_1 = |\mathcal{S}|$ and for each scenario $s \in \mathcal{S}$ its probability as unique element of $\Omega_s^{(1)}$ satisfies $p_{\Omega_s^{(1)}}^s = 1$, while the intra-level weights are given by $\pi_s^{(1)} = p^s$, according to (16) and (17), respectively. Third, the single-cut version of the L-shaped method can also be interpreted as a special case of our approach, corresponding to the top level $j = J$ of the refinement chain (10). However, the equivalence between the two formulations is not straightforward, as it requires proving that the optimality cuts (9c) and (24c) are equivalent. This result is established in the next section.

4.2 L-shaped method between consecutive levels of the refinement chain

In this section, we analyze the relationship among the optimality cuts (24c) obtained at two consecutive levels of the refinement chain (10). These results form the basis for proving the convergence of the proposed L-shaped refinement chain cuts method, established at the end of this section.

According to property (R2), suppose that at level $j \in \{2, \dots, J\}$ of the refinement chain, set $\Omega_i^{(j)}$, with $i \in \{1, \dots, m_j\}$, is the union of N_i subsets $\{\Omega_{k_\ell}^{(j-1)}\}_{\ell=1}^{N_i}$ from level $j-1$. The set $\Omega_i^{(j)}$ and each subset $\Omega_{k_\ell}^{(j-1)}$ are associated with a recourse problem (21), having corresponding dual feasible regions $\Lambda_i^{(j)} \subseteq \mathbb{R}^{p \cdot |\Omega_i^{(j)}|}$ and $\Lambda_{k_\ell}^{(j-1)} \subseteq \mathbb{R}^{p \cdot |\Omega_{k_\ell}^{(j-1)}|}$, respectively. In general, each $\Omega_{k_\ell}^{(j-1)}$ may contain a different number of scenarios, so its cardinality $|\Omega_{k_\ell}^{(j-1)}|$ may vary across the N_i subsets. However, since by construction $|\Omega_i^{(j)}| \geq |\Omega_{k_\ell}^{(j-1)}|$ for all $\ell = 1, \dots, N_i$ and therefore $p \cdot |\Omega_i^{(j)}| \geq p \cdot |\Omega_{k_\ell}^{(j-1)}|$, we assume that every point in each $\Lambda_{k_\ell}^{(j-1)}$ has exactly $p \cdot |\Omega_i^{(j)}|$ components. This can be obtained by setting to zero all components corresponding to scenarios not present in $\Omega_{k_\ell}^{(j-1)}$.

In Section 4.2.1, we examine the relationship between extreme points at consecutive levels of the refinement chain, while Section 4.2.2 focuses on the corresponding relationships between Benders cuts.

4.2.1 Relationship between extreme points

In the next two lemmas, we begin by examining the connections between the dual feasible region $\Lambda_i^{(j)}$ at level j with the collection of dual feasible regions $\{\Lambda_{k_\ell}^{(j-1)}\}_{\ell=1}^{N_i}$ at level $j-1$ of the refinement chain.

Lemma 2 Let $\{\lambda_{k_\ell}^{(j-1)}\}_{\ell=1}^{N_i}$ be a collection of points such that $\lambda_{k_\ell}^{(j-1)} \in \Lambda_{k_\ell}^{(j-1)}$ for all $\ell = 1, \dots, N_i$. Then:

$$\sum_{\ell=1}^{N_i} \pi_{k_\ell, i}^{(j-1, j)} \lambda_{k_\ell}^{(j-1)}$$

belongs to $\Lambda_i^{(j)}$.

Proof Let $\tilde{\lambda}_i^{(j)} := \sum_{\ell=1}^{N_i} \pi_{k_\ell, i}^{(j-1, j)} \lambda_{k_\ell}^{(j-1)}$. We need to show that $\tilde{\lambda}_i^{(j)}$ satisfies condition (22b). Consider scenario $\omega^s \in \Omega_i^{(j)}$. We have that:

$$\begin{aligned} \mathbf{W}^\top (\tilde{\lambda}_i^{(j)})^s &= \mathbf{W}^\top \sum_{\ell=1}^{N_i} \pi_{k_\ell, i}^{(j-1, j)} (\lambda_{k_\ell}^{(j-1)})^s \\ &= \sum_{\ell=1}^{N_i} \pi_{k_\ell, i}^{(j-1, j)} \left(\mathbf{W}^\top (\lambda_{k_\ell}^{(j-1)})^s \right). \end{aligned}$$

Since by hypothesis $\lambda_{k_\ell}^{(j-1)} \in \Lambda_{k_\ell}^{(j-1)}$, each $(\lambda_{k_\ell}^{(j-1)})^s$ satisfies condition (22b). Hence, we get:

$$\begin{aligned} \mathbf{W}^\top (\tilde{\lambda}_i^{(j)})^s &\leq \sum_{\ell=1}^{N_i} \pi_{k_\ell, i}^{(j-1, j)} p_{\Omega_{k_\ell}^{(j-1)}}^s \mathbf{q}^s \\ &= \mathbf{q}^s \sum_{\ell=1}^{N_i} \pi_{k_\ell, i}^{(j-1, j)} p_{\Omega_{k_\ell}^{(j-1)}}^s \\ &= p_{\Omega_i^{(j)}}^s \mathbf{q}^s, \end{aligned}$$

where the last equality follows from property (P3) of the refinement chain of probabilities. Therefore, $\tilde{\lambda}_i^{(j)}$ satisfies condition (22b), which proves the lemma. \square

This result implies that any convex combination of points in $\{\Lambda_{k_\ell}^{(j-1)}\}_{\ell=1}^{N_i}$ with coefficients given by the inter-level weights $\{\pi_{k_\ell, i}^{(j-1, j)}\}_{\ell=1}^{N_i}$ belongs to $\Lambda_i^{(j)}$. Conversely, in the two cases discussed in Section 3 for the construction of the refinement chain (fixed scenarios and disjoint partitions), each point in $\Lambda_i^{(j)}$ can be characterized as a convex combination of points in $\{\Lambda_{k_\ell}^{(j-1)}\}_{\ell=1}^{N_i}$, as shown in the following lemma.

Lemma 3 Suppose that the subsets $\{\Omega_{k_\ell}^{(j-1)}\}_{\ell=1}^{N_i}$ are either disjoint or with fixed scenarios appearing in all of them. Then, for each $\lambda_i^{(j)} \in \Lambda_i^{(j)}$ there exists a collection of points $\{\lambda_{k_\ell}^{(j-1)}\}_{\ell=1}^{N_i}$ with $\lambda_{k_\ell}^{(j-1)} \in \Lambda_{k_\ell}^{(j-1)}$ for all $\ell = 1, \dots, N_i$ such that:

$$\sum_{\ell=1}^{N_i} \pi_{k_\ell, i}^{(j-1, j)} \lambda_{k_\ell}^{(j-1)} = \lambda_i^{(j)}. \quad (25)$$

Proof We discuss the two cases separately.

In the first case, suppose that subsets $\{\Omega_{k_\ell}^{(j-1)}\}_{\ell=1}^{N_i}$ are disjoint. This implies that each scenario $\omega^s \in \Omega_i^{(j)}$ appears in one and only one subset $\Omega_{k_{\bar{\ell}(s)}}^{(j-1)}$ at level $j-1$, with $\bar{\ell}(s) \in \{1, \dots, N_i\}$. For each $\omega^s \in \Omega_i^{(j)}$, we can consider:

$$(\boldsymbol{\lambda}_{k_\ell}^{(j-1)})^s := \begin{cases} \frac{1}{\pi_{k_\ell, i}^{(j-1, j)}} (\boldsymbol{\lambda}_i^{(j)})^s & \text{if } \ell = \bar{\ell}(s) \\ 0 & \text{if } \ell \neq \bar{\ell}(s). \end{cases} \quad (26)$$

First, we need to show that the collection of points defined according (26) satisfies $\boldsymbol{\lambda}_{k_\ell}^{(j-1)} \in \Lambda_{k_\ell}^{(j-1)}$ for all $\ell = 1, \dots, N_i$. Consider a scenario $\omega^s \in \Omega_i^{(j)}$ with corresponding unique subset $\Omega_{k_{\bar{\ell}(s)}}^{(j-1)} \ni \omega^s$. For all subsets $\Omega_{k_\ell}^{(j-1)}$ with $\ell \neq \bar{\ell}(s)$, it follows that $(\boldsymbol{\lambda}_{k_\ell}^{(j-1)})^s = \mathbf{0}$, and therefore condition (22b) is automatically satisfied by setting $p_{\Omega_{k_\ell}^{(j-1)}}^s = 0$. Conversely, for the subset $\Omega_{k_{\bar{\ell}(s)}}^{(j-1)}$, we have that:

$$\mathbf{W}^\top (\boldsymbol{\lambda}_{k_{\bar{\ell}(s)}}^{(j-1)})^s = \frac{1}{\pi_{k_{\bar{\ell}(s)}, i}^{(j-1, j)}} \mathbf{W}^\top (\boldsymbol{\lambda}_i^{(j)})^s \leq \frac{1}{\pi_{k_{\bar{\ell}(s)}, i}^{(j-1, j)}} p_{\Omega_i^{(j)}}^s \mathbf{q}^s, \quad (27)$$

where the last inequality holds because $(\boldsymbol{\lambda}_i^{(j)})^s \in (\Lambda_i^{(j)})^s$. Moreover, combining (18) with (16)–(17), the right-hand side of (27) can be reformulated as:

$$\begin{aligned} \frac{1}{\pi_{k_{\bar{\ell}(s)}, i}^{(j-1, j)}} p_{\Omega_i^{(j)}}^s \mathbf{q}^s &= \frac{\pi_i^{(j)}}{\pi_{k_{\bar{\ell}(s)}}^{(j-1)}} \cdot \frac{1}{\pi_i^{(j)}} p^s \mathbf{q}^s \\ &= \frac{1}{\pi_{k_{\bar{\ell}(s)}}^{(j-1)}} \cdot p_{\Omega_{k_{\bar{\ell}(s)}}^{(j-1)}}^s \pi_{k_{\bar{\ell}(s)}}^{(j-1)} \mathbf{q}^s \\ &= p_{\Omega_{k_{\bar{\ell}(s)}}^{(j-1)}}^s \mathbf{q}^s. \end{aligned}$$

Therefore, $\mathbf{W}^\top (\boldsymbol{\lambda}_{k_{\bar{\ell}(s)}}^{(j-1)})^s \leq p_{\Omega_{k_{\bar{\ell}(s)}}^{(j-1)}}^s \mathbf{q}^s$, or, equivalently, $(\boldsymbol{\lambda}_{k_{\bar{\ell}(s)}}^{(j-1)})^s \in (\Lambda_{k_{\bar{\ell}(s)}}^{(j-1)})^s$. Second, it remains to prove that the collection $\{\boldsymbol{\lambda}_{k_\ell}^{(j-1)}\}_{\ell=1}^{N_i}$ satisfies (25). To verify this, note that for all scenarios $\omega^s \in \Omega_i^{(j-1)}$, it holds that:

$$\sum_{\ell=1}^{N_i} \pi_{k_\ell, i}^{(j-1, j)} (\boldsymbol{\lambda}_{k_\ell}^{(j-1)})^s = \pi_{k_{\bar{\ell}(s)}, i}^{(j-1, j)} (\boldsymbol{\lambda}_{k_{\bar{\ell}(s)}}^{(j-1)})^s = \pi_{k_{\bar{\ell}(s)}, i}^{(j-1, j)} \cdot \frac{1}{\pi_{k_{\bar{\ell}(s)}, i}^{(j-1, j)}} (\boldsymbol{\lambda}_i^{(j)})^s = (\boldsymbol{\lambda}_i^{(j)})^s.$$

In the second case, suppose that all subsets $\{\Omega_{k_\ell}^{(j-1)}\}_{\ell=1}^{N_i}$ have the first $f \geq 1$ scenarios fixed, appearing in all of them. By property (R2), these f scenarios are also fixed in $\Omega_i^{(j)}$, since $\Omega_i^{(j)}$ is the union of the subsets $\{\Omega_{k_\ell}^{(j-1)}\}_{\ell=1}^{N_i}$. Therefore, for all $s = 1, \dots, f$, it is sufficient to set:

$$(\boldsymbol{\lambda}_{k_\ell}^{(j-1)})^s := (\boldsymbol{\lambda}_i^{(j)})^s \quad \forall \ell = 1, \dots, N_i.$$

By construction, all remaining and non-fixed scenarios appear in one and only one subset $\Omega_{k_{\bar{\ell}(s)}}^{(j-1)}$, with $\bar{\ell}(s) \in \{1, \dots, N_i\}$. Therefore, for all $s = f+1, \dots, |\Omega_i^{(j)}|$, we can define $(\boldsymbol{\lambda}_{k_\ell}^{(j-1)})^s$ as in (26).

For the fixed scenarios, condition (22b) is satisfied, because probability $p_{\Omega_i^{(j)}}^s = p^s$ for all $s = 1, \dots, f$ (see (14)). For the non-fixed scenario, the proof is analogous to the case of disjoint subsets discussed above. Regarding condition (25), for all fixed scenarios $s = 1, \dots, f$, it holds that:

$$\sum_{\ell=1}^{N_i} \pi_{k_\ell, i}^{(j-1, j)} (\boldsymbol{\lambda}_{k_\ell}^{(j-1)})^s = \sum_{\ell=1}^{N_i} \pi_{k_\ell, i}^{(j-1, j)} (\boldsymbol{\lambda}_i^{(j)})^s = (\boldsymbol{\lambda}_i^{(j)})^s \sum_{\ell=1}^{N_i} \pi_{k_\ell, i}^{(j-1, j)} = (\boldsymbol{\lambda}_i^{(j)})^s,$$

where the last equality follows from property (P2) on the intra-level weights. Finally, for all remaining scenarios, we have that:

$$\sum_{\ell=1}^{N_i} \pi_{k_\ell, i}^{(j-1, j)} (\boldsymbol{\lambda}_{k_\ell}^{(j-1)})^s = \pi_{k_{\bar{\ell}}, i}^{(j-1, j)} (\boldsymbol{\lambda}_{k_{\bar{\ell}}}^{(j-1)})^s = \pi_{k_{\bar{\ell}}, i}^{(j-1, j)} \cdot \frac{1}{\pi_{k_{\bar{\ell}}, i}^{(j-1, j)}} (\boldsymbol{\lambda}_i^{(j)})^s = (\boldsymbol{\lambda}_i^{(j)})^s.$$

This concludes the proof. \square

In the construction of the optimality cuts (24c), the extreme points of the dual feasible region $\Lambda_i^{(j)}$ at level j are considered. The following proposition establishes a connection between the extreme points of $\Lambda_i^{(j)}$ at level j and those of the collection $\{\Lambda_{k_\ell}^{(j-1)}\}_{\ell=1}^{N_i}$ at level $j-1$.

Proposition 4 *Suppose that the subsets $\{\Omega_{k_\ell}^{(j-1)}\}_{\ell=1}^{N_i}$ are either disjoint or with fixed scenarios appearing in all of them. Let $\{\mathbf{e}_{k_\ell}^{(j-1)}\}_{\ell=1}^{N_i}$ be a collection of points such that $\mathbf{e}_{k_\ell}^{(j-1)} \in \Lambda_{k_\ell}^{(j-1)}$ for all $\ell = 1, \dots, N_i$, with corresponding objective function values in (22a) denoted by $\{z_{k_\ell}^{(j-1)}\}_{\ell=1}^{N_i}$. Then:*

$$\mathbf{e}_i^{(j)} := \sum_{\ell=1}^{N_i} \pi_{k_\ell, i}^{(j-1, j)} \mathbf{e}_{k_\ell}^{(j-1)} \quad (28)$$

is an extreme point of $\Lambda_i^{(j)}$ if and only if each $\mathbf{e}_{k_\ell}^{(j-1)}$ is an extreme point of $\Lambda_{k_\ell}^{(j-1)}$ for all $\ell = 1, \dots, N_i$. In this case, the corresponding objective function value $z_i^{(j)}$ satisfies:

$$z_i^{(j)} = \sum_{\ell=1}^{N_i} \pi_{k_\ell, i}^{(j-1, j)} z_{k_\ell}^{(j-1)}.$$

Proof By Lemma 2, the point $\mathbf{e}_i^{(j)}$ belongs to $\Lambda_i^{(j)}$, since it is defined as a convex combination of points in $\{\Lambda_{k_\ell}^{(j-1)}\}_{\ell=1}^{N_i}$ with weights $\{\pi_{k_\ell, i}^{(j-1, j)}\}_{\ell=1}^{N_i}$.

We first prove the forward implication. Suppose that each $\mathbf{e}_{k_\ell}^{(j-1)}$ is an extreme point of $\Lambda_{k_\ell}^{(j-1)}$ for all $\ell = 1, \dots, N_i$. Assume, by contradiction, that $\mathbf{e}_i^{(j)}$ is not an extreme point of $\Lambda_i^{(j)}$. Then, there exist distinct points $\tilde{\mathbf{e}}_i^{(j)}, \hat{\mathbf{e}}_i^{(j)} \in \Lambda_i^{(j)}$, with $\tilde{\mathbf{e}}_i^{(j)}, \hat{\mathbf{e}}_i^{(j)} \neq \mathbf{e}_i^{(j)}$ and $\alpha \in (0, 1)$ such that $\mathbf{e}_i^{(j)} = \alpha \tilde{\mathbf{e}}_i^{(j)} + (1 - \alpha) \hat{\mathbf{e}}_i^{(j)}$. By Lemma 3, since $\tilde{\mathbf{e}}_i^{(j)}, \hat{\mathbf{e}}_i^{(j)} \in \Lambda_i^{(j)}$, there exist two collections $\{\tilde{\mathbf{e}}_{k_\ell}^{(j-1)}\}_{\ell=1}^{N_i}, \{\hat{\mathbf{e}}_{k_\ell}^{(j-1)}\}_{\ell=1}^{N_i}$ with $\tilde{\mathbf{e}}_{k_\ell}^{(j-1)}, \hat{\mathbf{e}}_{k_\ell}^{(j-1)} \in \Lambda_{k_\ell}^{(j-1)}$ for all $\ell = 1, \dots, N_i$ such that:

$$\tilde{\mathbf{e}}_i^{(j)} = \sum_{\ell=1}^{N_i} \pi_{k_\ell, i}^{(j-1, j)} \tilde{\mathbf{e}}_{k_\ell}^{(j-1)} \quad \text{and} \quad \hat{\mathbf{e}}_i^{(j)} = \sum_{\ell=1}^{N_i} \pi_{k_\ell, i}^{(j-1, j)} \hat{\mathbf{e}}_{k_\ell}^{(j-1)}.$$

Therefore, we can re-write $\mathbf{e}_i^{(j)}$ as:

$$\begin{aligned}\mathbf{e}_i^{(j)} &= \alpha \sum_{\ell=1}^{N_i} \pi_{k_\ell, i}^{(j-1, j)} \tilde{\mathbf{e}}_{k_\ell}^{(j-1)} + (1 - \alpha) \sum_{\ell=1}^{N_i} \pi_{k_\ell, i}^{(j-1, j)} \hat{\mathbf{e}}_{k_\ell}^{(j-1)} \\ &= \sum_{\ell=1}^{N_i} \pi_{k_\ell, i}^{(j-1, j)} [\alpha \tilde{\mathbf{e}}_{k_\ell}^{(j-1)} + (1 - \alpha) \hat{\mathbf{e}}_{k_\ell}^{(j-1)}]\end{aligned}$$

Comparing this expression with (28) we obtain $\mathbf{e}_{k_\ell}^{(j-1)} = \alpha \tilde{\mathbf{e}}_{k_\ell}^{(j-1)} + (1 - \alpha) \hat{\mathbf{e}}_{k_\ell}^{(j-1)}$ for all $\ell = 1, \dots, N_i$. This contradicts the assumption that each $\mathbf{e}_{k_\ell}^{(j-1)}$ is an extreme point of $\Lambda_{k_\ell}^{(j-1)}$.

We now prove the converse implication. Suppose that $\mathbf{e}_i^{(j)}$ is an extreme point of $\mathcal{E}(\Lambda_i^{(j)})$. Fix $\ell \in \{1, \dots, N_i\}$ and assume, by contradiction, that $\mathbf{e}_{k_\ell}^{(j-1)}$ is not an extreme point of $\Lambda_{k_\ell}^{(j-1)}$. Then, there exist distinct points $\tilde{\mathbf{e}}_{k_\ell}^{(j-1)}$ and $\bar{\mathbf{e}}_{k_\ell}^{(j-1)}$ in $\Lambda_{k_\ell}^{(j-1)}$ with $\tilde{\mathbf{e}}_{k_\ell}^{(j-1)}, \bar{\mathbf{e}}_{k_\ell}^{(j-1)} \neq \mathbf{e}_{k_\ell}^{(j-1)}$ and $\alpha \in (0, 1)$ such that $\mathbf{e}_{k_\ell}^{(j-1)} = \alpha \tilde{\mathbf{e}}_{k_\ell}^{(j-1)} + (1 - \alpha) \bar{\mathbf{e}}_{k_\ell}^{(j-1)}$. Therefore, substituting into (28) yields:

$$\begin{aligned}\mathbf{e}_i^{(j)} &= \sum_{\ell=1}^{N_i} \pi_{k_\ell, i}^{(j-1, j)} \mathbf{e}_{k_\ell}^{(j-1)} \\ &= \sum_{\ell=1}^{N_i} \pi_{k_\ell, i}^{(j-1, j)} [\alpha \tilde{\mathbf{e}}_{k_\ell}^{(j-1)} + (1 - \alpha) \bar{\mathbf{e}}_{k_\ell}^{(j-1)}] \\ &= \alpha \sum_{\ell=1}^{N_i} \pi_{k_\ell, i}^{(j-1, j)} \tilde{\mathbf{e}}_{k_\ell}^{(j-1)} + (1 - \alpha) \sum_{\ell=1}^{N_i} \pi_{k_\ell, i}^{(j-1, j)} \bar{\mathbf{e}}_{k_\ell}^{(j-1)}.\end{aligned}$$

By Lemma 2, each summation on the last right-hand side defines a point in Λ_i^j . Consequently, $\mathbf{e}_i^{(j)}$ is not an extreme point of Λ_i^j , which contradicts the assumption.

Finally, we evaluate the objective function (22a) at $\mathbf{e}_i^{(j)}$:

$$\begin{aligned}z_i^{(j)} &= \sum_{s: \boldsymbol{\omega}^s \in \Omega_i^{(j)}} (\mathbf{h}^s - \mathbf{T}^s \mathbf{x})^\top (\mathbf{e}_i^{(j)})^s \\ &= \sum_{s: \boldsymbol{\omega}^s \in \Omega_i^{(j)}} (\mathbf{h}^s - \mathbf{T}^s \mathbf{x})^\top \sum_{\ell=1}^{N_i} \pi_{k_\ell, i}^{(j-1, j)} (\mathbf{e}_{k_\ell}^{(j-1)})^s \\ &= \sum_{\ell=1}^{N_i} \pi_{k_\ell, i}^{(j-1, j)} \sum_{s: \boldsymbol{\omega}^s \in \Omega_i^{(j)}} (\mathbf{h}^s - \mathbf{T}^s \mathbf{x})^\top (\mathbf{e}_{k_\ell}^{(j-1)})^s \\ &= \sum_{\ell=1}^{N_i} \pi_{k_\ell, i}^{(j-1, j)} \sum_{s: \boldsymbol{\omega}^s \in \Omega_{k_\ell}^{(j-1)}} (\mathbf{h}^s - \mathbf{T}^s \mathbf{x})^\top (\mathbf{e}_{k_\ell}^{(j-1)})^s \\ &= \sum_{\ell=1}^{N_i} \pi_{k_\ell, i}^{(j-1, j)} z_{k_\ell}^{(j-1)},\end{aligned}$$

where the fourth equality follows from property (R2) of the refinement chain.

This concludes the proof. \square

Thanks to Proposition 4, we can show that the single-cut version of the L-shaped approach [57] can be interpreted as a special case of our L-shaped refinement chain cuts method. This equivalence is formally stated and proved in the following corollary.

Corollary 5 *Consider a refinement chain with J levels, composed either of disjoint subsets or of subsets with fixed scenarios. Then, the single-cut optimality cut (9c) coincides with the optimality cut (24c) at the top level J .*

Proof Assume that at level 1 of the refinement chain each subset contains a single scenario. Note that, in the case of a refinement chain with fixed scenarios, it is always possible to introduce an additional bottom level consisting of single-scenario subsets, so this assumption is without loss of generality.

At level J , we have $\Omega_1^J = \Omega$. Consequently, in (24c) it holds that $\mathbf{h}_1^{(J)} = \mathbf{h}$, $\mathbf{T}_1^{(J)} = \mathbf{T}$, and $\theta_1^{(J)} = \Theta$. Therefore, to establish the equivalence between (9c) and (24c), it suffices to show that $\sum_{s \in \mathcal{S}} p^s e^s$, where e^s are extreme points at the bottom level, is an extreme point of $\Lambda_1^{(J)}$.

Since single scenarios appear at level 1 of the refinement chain, we have $m_1 = |\mathcal{S}|$, and, from (17), it follows that $p^s = \pi_s^{(1)}$ for all $s \in \mathcal{S}$. Considering levels 1 and 2 and applying (18), we obtain:

$$\begin{aligned} \sum_{s \in \mathcal{S}} p^s e^s &= \sum_{s=1}^{m_1} \pi_s^{(1)} e^s \\ &= \sum_{s_2=1}^{m_2} \sum_{s: \Omega_s^{(1)} \subseteq \Omega_{s_2}^{(2)}} \pi_s^{(1)} e^s \\ &= \sum_{s_2=1}^{m_2} \sum_{s: \Omega_s^{(1)} \subseteq \Omega_{s_2}^{(2)}} \pi_{s, s_2}^{(1,2)} \pi_{s_2}^{(2)} e^s \\ &= \sum_{s_2=1}^{m_2} \pi_{s_2}^{(2)} \sum_{s: \Omega_s^{(1)} \subseteq \Omega_{s_2}^{(2)}} \pi_{s, s_2}^{(1,2)} e^s \\ &= \sum_{s_2=1}^{m_2} \pi_{s_2}^{(2)} e_{s_2}^{(2)}, \end{aligned}$$

where, in the last equality, we applied Proposition 4, since $e_{s_2}^{(2)} := \sum_{s: \Omega_s^{(1)} \subseteq \Omega_{s_2}^{(2)}} \pi_{s, s_2}^{(1,2)} e^s$ is an extreme point of $\Lambda_{s_2}^{(2)}$, with $s_2 \in \{1, \dots, m_2\}$. The same procedure can be applied recursively along the refinement chain up to level $J-1$. At level J , there is a single set $\Omega_1^{(J)} = \Omega$, whose unique intra-level weight satisfies $\pi_1^{(J)} = 1$ by property (P2). Applying (18) yields:

$$\sum_{s \in \mathcal{S}} p^s e^s = \sum_{s_{J-1}=1}^{m_{J-1}} \pi_{s_{J-1}}^{(J-1)} e_{s_{J-1}}^{(J-1)} = \sum_{s_{J-1}=1}^{m_{J-1}} \pi_{s_{J-1}, 1}^{(J-1, J)} e_{s_{J-1}}^{(J-1)},$$

which, by Proposition 4, is an extreme point of $\Lambda_1^{(J)}$. This completes the proof. \square

In the following proposition, we establish the relationship between optimal extreme points at level $j-1$ and those at level j of the refinement chain.

Proposition 6 Suppose that the subsets $\{\Omega_{k_\ell}^{(j-1)}\}_{\ell=1}^{N_i}$ are either disjoint or with fixed scenarios appearing in all of them. Let $\{e_{k_\ell}^{(j-1)}\}_{\ell=1}^{N_i}$ be a collection of extreme points such that $e_{k_\ell}^{(j-1)} \in \mathcal{E}(\Lambda_{k_\ell}^{(j-1)})$ for all $\ell = 1, \dots, N_i$, with corresponding objective function values (22a) denoted by $\{z_{k_\ell}^{(j-1)}\}_{\ell=1}^{N_i}$. Then:

$$e_i^{(j)} := \sum_{\ell=1}^{N_i} \pi_{k_\ell, i}^{(j-1, j)} e_{k_\ell}^{(j-1)} \quad (29)$$

is an optimal extreme point of problem (22) at level j if and only if each $e_{k_\ell}^{(j-1)}$ is an optimal extreme point of the corresponding problem at level $j-1$ for all $\ell = 1, \dots, N_i$.

Proof By Proposition 4, the point $e_i^{(j)}$ defined in (29) is an extreme point of the dual feasible region $\Lambda_i^{(j)}$ at level j . Let $z_i^{(j)}$ denote its associated objective function value.

We first prove the forward implication. Suppose that each $e_{k_\ell}^{(j-1)}$ is an optimal extreme point of $\Lambda_{k_\ell}^{(j-1)}$ for all $\ell = 1, \dots, N_i$. Assume, by contradiction, that there exists another extreme point $\tilde{e}_i^{(j)} \in \Lambda_i^{(j)}$ with objective function value $\tilde{z}_i^{(j)} > z_i^{(j)}$. By Proposition 4, there exists a collection $\{\tilde{e}_{k_\ell}^{(j-1)}\}_{\ell=1}^{N_i}$, with $\tilde{e}_{k_\ell}^{(j-1)} \in \Lambda_{k_\ell}^{(j-1)}$, for all $\ell = 1, \dots, N_i$, such that $\tilde{e}_i^{(j)} = \sum_{\ell=1}^{N_i} \pi_{k_\ell, i}^{(j-1, j)} \tilde{e}_{k_\ell}^{(j-1)}$, with corresponding objective function values $\tilde{z}_{k_\ell}^{(j-1)}$ satisfying $\tilde{z}_i^{(j)} = \sum_{\ell=1}^{N_i} \pi_{k_\ell, i}^{(j-1, j)} \tilde{z}_{k_\ell}^{(j-1)}$. Hence, by the assumption of contradiction, it holds that:

$$\tilde{z}_i^{(j)} - z_i^{(j)} = \sum_{\ell=1}^{N_i} \pi_{k_\ell, i}^{(j-1, j)} [\tilde{z}_{k_\ell}^{(j-1)} - z_{k_\ell}^{(j-1)}] > 0.$$

This is not possible since all inter-level weights $\pi_{k_\ell, i}^{(j-1, j)}$ are non-negative and each $z_{k_\ell}^{(j-1)}$ is assumed to be optimal, implying $z_{k_\ell}^{(j-1)} > \tilde{z}_{k_\ell}^{(j-1)}$ for all $\ell = 1, \dots, N_i$.

We now prove the reverse implication. Suppose that $e_i^{(j)}$ is an optimal extreme point of problem (22) at level j , with objective function value $z_i^{(j)}$. Assume by contradiction that there exists an index $\bar{\ell} \in \{1, \dots, N_i\}$ and an extreme point $\tilde{e}_{k_{\bar{\ell}}}^{(j-1)}$ such that $\tilde{z}_{k_{\bar{\ell}}}^{(j-1)} > z_{k_{\bar{\ell}}}^{(j-1)}$. Then, defining $\tilde{e}_i^{(j)}$ as:

$$\tilde{e}_i^{(j)} := \pi_{k_{\bar{\ell}}, i}^{(j-1, j)} \tilde{e}_{k_{\bar{\ell}}}^{(j-1)} + \sum_{\ell=1, \ell \neq \bar{\ell}}^{N_i} \pi_{k_\ell, i}^{(j-1, j)} e_{k_\ell}^{(j-1)},$$

the associated objective function value $\tilde{z}_i^{(j)}$ satisfies:

$$\tilde{z}_i^{(j)} = \pi_{k_{\bar{\ell}}, i}^{(j-1, j)} \tilde{z}_{k_{\bar{\ell}}}^{(j-1)} + \sum_{\ell=1, \ell \neq \bar{\ell}}^{N_i} \pi_{k_\ell, i}^{(j-1, j)} z_{k_\ell}^{(j-1)} > \pi_{k_{\bar{\ell}}, i}^{(j-1, j)} z_{k_{\bar{\ell}}}^{(j-1)} + \sum_{\ell=1, \ell \neq \bar{\ell}}^{N_i} \pi_{k_\ell, i}^{(j-1, j)} z_{k_\ell}^{(j-1)} = z_i^{(j)}, \quad (30)$$

contradicting the optimality of $e_i^{(j)}$.

This concludes the proof. \square

4.2.2 Relationship between Benders cuts

In this section, we investigate the relationship between consecutive levels $j-1$ and j of the refinement chain in terms of Benders cuts. We begin by establishing the connection between the corresponding optimality cuts in the following proposition.

Proposition 7 *Suppose that subsets $\{\Omega_{k_\ell}^{(j-1)}\}_{\ell=1}^{N_i}$ are either disjoint or with fixed scenarios appearing in all of them. Let $\{\mathbf{e}_{k_\ell}^{(j-1)}\}_{\ell=1}^{N_i}$ be a collection of extreme points such that $\mathbf{e}_{k_\ell}^{(j-1)} \in \mathcal{E}(\Lambda_{k_\ell}^{(j-1)})$ for all $\ell = 1, \dots, N_i$. Then:*

$$(\mathbf{h}_i^{(j)} - \mathbf{T}_i^{(j)} \mathbf{x})^\top \sum_{\ell=1}^{N_i} \pi_{k_\ell, i}^{(j-1, j)} \mathbf{e}_{k_\ell}^{(j-1)} \leq \theta_i^{(j)} \quad (31)$$

is an optimality cut for Problem (24) defined over the set $\Omega_i^{(j)}$.

Proof Consider the collection of optimality cuts $(\mathbf{h}_{k_\ell}^{(j-1)} - \mathbf{T}_{k_\ell}^{(j-1)} \mathbf{x})^\top \mathbf{e}_{k_\ell}^{(j-1)} \leq \theta_{k_\ell}^{(j-1)}$, one for each subset $\Omega_{k_\ell}^{(j-1)}$, with $\ell = 1, \dots, N_i$. If $\mathbf{x} \in \mathcal{X}$ satisfies all these inequalities, then it must also satisfy:

$$\sum_{\ell=1}^{N_i} \pi_{k_\ell, i}^{(j-1, j)} (\mathbf{h}_{k_\ell}^{(j-1)} - \mathbf{T}_{k_\ell}^{(j-1)} \mathbf{x})^\top \mathbf{e}_{k_\ell}^{(j-1)} \leq \sum_{\ell=1}^{N_i} \pi_{k_\ell, i}^{(j-1, j)} \theta_{k_\ell}^{(j-1)}. \quad (32)$$

Here, we have assumed that the components corresponding to scenarios not present in $\Omega_{k_\ell}^{(j-1)}$ are set to zero, so that $\mathbf{h}_{k_\ell}^{(j-1)} \in \mathbb{R}^{p \cdot |\Omega_i^{(j)}|}$ and $\mathbf{T}_{k_\ell}^{(j-1)} \in \mathbb{R}^{p \cdot |\Omega_i^{(j)}| \times n}$ for all $k_\ell = 1, \dots, N_i$. Therefore, the left hand-side of (32) can be re-written as:

$$\sum_{\ell=1}^{N_i} \pi_{k_\ell, i}^{(j-1, j)} (\mathbf{h}_i^{(j)} - \mathbf{T}_i^{(j)} \mathbf{x})^\top \mathbf{e}_{k_\ell}^{(j-1)} = (\mathbf{h}_i^{(j)} - \mathbf{T}_i^{(j)} \mathbf{x})^\top \sum_{\ell=1}^{N_i} \pi_{k_\ell, i}^{(j-1, j)} \mathbf{e}_{k_\ell}^{(j-1)}. \quad (33)$$

By Proposition 4, the summation in the right-hand side of (33) defines an extreme point of $\Lambda_i^{(j)}$.

It remains to prove the relationship between $\theta_i^{(j)}$ and $\sum_{\ell=1}^{N_i} \pi_{k_\ell, i}^{(j-1, j)} \theta_{k_\ell}^{(j-1)}$, i.e., between the right-hand side of (31) and (32), respectively. From (18), we have that:

$$\sum_{\ell=1}^{N_i} \pi_{k_\ell, i}^{(j-1, j)} \theta_{k_\ell}^{(j-1)} = \sum_{\ell=1}^{N_i} \frac{\pi_{k_\ell}^{(j-1)}}{\pi_i^{(j)}} \theta_{k_\ell}^{(j-1)} = \frac{1}{\pi_i^{(j)}} \sum_{\ell=1}^{N_i} \pi_{k_\ell}^{(j-1)} \theta_{k_\ell}^{(j-1)}.$$

Since $\Omega_{k_\ell}^{(j-1)} \subseteq \Omega_i^{(j)}$ for all $\ell = 1, \dots, N_i$, it follows that $\theta_{k_\ell}^{(j-1)} \leq \theta_i^{(j)}$. Indeed, each θ represents an upper bound on the optimal value of the recourse problem $\mathcal{Q}(\cdot, \cdot)$, and the feasible region may shrink when moving from $\Omega_{k_\ell}^{(j-1)}$ to $\Omega_i^{(j)}$, as potentially more constraints (21b) are included. Therefore:

$$\frac{1}{\pi_i^{(j)}} \sum_{\ell=1}^{N_i} \pi_{k_\ell}^{(j-1)} \theta_{k_\ell}^{(j-1)} \leq \frac{1}{\pi_i^{(j)}} \sum_{\ell=1}^{N_i} \pi_{k_\ell}^{(j-1)} \theta_i^{(j)} = \theta_i^{(j)} \frac{1}{\pi_i^{(j)}} \sum_{\ell=1}^{N_i} \pi_{k_\ell}^{(j-1)} = \theta_i^{(j)}, \quad (34)$$

where the last equality follows from (19). Combining (32)–(33) with (34), we obtain that:

$$(\mathbf{h}_i^{(j)} - \mathbf{T}_i^{(j)} \mathbf{x})^\top \sum_{\ell=1}^{N_i} \pi_{k_\ell, i}^{(j-1, j)} \mathbf{e}_{k_\ell}^{(j-1)} \leq \sum_{\ell=1}^{N_i} \pi_{k_\ell, i}^{(j-1, j)} \theta_{k_\ell}^{(j-1)} \leq \theta_i^{(j)}.$$

This completes the proof. \square

Proposition 7 establishes how to construct an optimality cut at level j from optimality cuts at level $j - 1$. The following result further characterizes the relationship between consecutive levels.

Proposition 8 *Suppose that subsets $\{\Omega_{k_\ell}^{(j-1)}\}_{\ell=1}^{N_i}$ are either disjoint or with fixed scenarios appearing in all of them. Then, the left-hand side of the optimality cut (24c) at level j can be decomposed into a convex combination of left-hand sides of the corresponding optimality cuts at level $j - 1$, with weights $\pi_{k_\ell, i}^{(j-1, j)}$.*

Proof Let $\mathbf{e}_i^{(j)} \in \mathcal{E}(\Lambda_i^{(j)})$ be an extreme point at level j of the refinement chain. Thanks to Proposition 4, $\mathbf{e}_i^{(j)}$ can be decomposed as a convex combination of extreme points $\{\mathbf{e}_{k_\ell}^{(j-1)}\}_{\ell=1}^{N_i}$ at level $j - 1$ with weights $\{\pi_{k_\ell, i}^{(j-1, j)}\}_{\ell=1}^{N_i}$. Thus, the left-hand side of the optimality cut (24c) at level j can be re-written as:

$$\begin{aligned} (\mathbf{h}_i^{(j)} - \mathbf{T}_i^{(j)} \mathbf{x})^\top \mathbf{e}_i^{(j)} &= (\mathbf{h}_i^{(j)} - \mathbf{T}_i^{(j)} \mathbf{x})^\top \sum_{\ell=1}^{N_i} \pi_{k_\ell, i}^{(j-1, j)} \mathbf{e}_{k_\ell}^{(j-1)} \\ &= \sum_{\ell=1}^{N_i} \pi_{k_\ell, i}^{(j-1, j)} [(\mathbf{h}_i^{(j)} - \mathbf{T}_i^{(j)} \mathbf{x})^\top \mathbf{e}_{k_\ell}^{(j-1)}]. \end{aligned}$$

Since each $\mathbf{e}_{k_\ell}^{(j-1)}$ has zero components for all scenarios not contained in $\Omega_i^{(j)}$, the scalar product reduces to the terms associated with scenarios in $\Omega_i^{(j)}$, while all remaining terms vanish. Thus, the retained terms are the ones related to $\mathbf{h}_{k_\ell}^{(j-1)}$ and $\mathbf{T}_{k_\ell}^{(j-1)}$. Thus:

$$(\mathbf{h}_i^{(j)} - \mathbf{T}_i^{(j)} \mathbf{x})^\top \mathbf{e}_i^{(j)} = \sum_{\ell=1}^{N_i} \pi_{k_\ell, i}^{(j-1, j)} [(\mathbf{h}_{k_\ell}^{(j-1)} - \mathbf{T}_{k_\ell}^{(j-1)} \mathbf{x})^\top \mathbf{e}_{k_\ell}^{(j-1)}].$$

The term in square brackets corresponds the left-hand side of the optimality cut (24c) at level $j - 1$. This concludes the proof. \square

When considering the extreme rays and the corresponding feasibility cuts across consecutive levels, results analogous to those stated in Propositions 4–6 and 7–8 do not hold. Indeed, the extreme rays and feasibility cuts remain identical at each level to those of the classical L-shaped method. This is formally established in the following result.

Proposition 9 *Let $\mathbf{r} \in \mathbb{R}^p$ be an extreme ray of Λ , with the associated set of feasibility cuts (8b). Then, the extreme rays of $\Lambda_i^{(j)}$ take the following form:*

$$\mathbf{r}^s := (\mathbf{b}^s \otimes \mathbf{I}_p) \mathbf{r} \quad \forall s : \omega^s \in \Omega_i^{(j)}, \quad (35)$$

where \mathbf{b}^s is the s -th standard basis vector of $\mathbb{R}^{|\Omega_i^{(j)}|}$, \mathbf{I}_p is the $p \times p$ identity matrix, and \otimes denotes the Kronecker product. Moreover, the feasibility cuts (24b) associated with r^s coincide with those in (8b).

Proof First, observe that vector \mathbf{r} is an extreme ray of $(\Lambda_i^{(j)})^s$ for all scenarios s in $\Omega_i^{(j)}$. Indeed, the dual feasible regions $(\Lambda_i^{(j)})^s$ and Λ differ only by a positive scalar multiple of \mathbf{q}^s in the right-hand side of inequalities (22b) and (5b), i.e., $p_{\Omega_i^{(j)}}^s \mathbf{q}^s$ versus \mathbf{q}^s . Hence, the direction of the extreme ray is not altered.

Next, by definition of \mathbf{r}^s in (35), the p components corresponding to scenario s coincide exactly with those of \mathbf{r} , while all remaining components are zero. Since $\Lambda_i^{(j)}$ is defined in (23) as the Cartesian product of the dual feasible regions $(\Lambda_i^{(j)})^s$, the extreme ray \mathbf{r}^s retains the same direction as \mathbf{r} . In this sense, \mathbf{r}^s can be considered as the projection of \mathbf{r} over $(\Lambda_i^{(j)})^s$.

Finally, in the feasibility cut (24b), only the components associated with scenario ω^s contribute, yielding the same formulation as in (8b). This completes the proof. \square

In the following example, we illustrate the theoretical results developed thus far.

Example 1 Consider the following two-stage stochastic optimization problem:

$$\min_{x, y_1^s, y_2^s} -x + \sum_{s=1}^5 p^s (-2y_1^s - y_2^s) \quad (36a)$$

$$\text{s.t. } y_1^1 + 2y_2^1 = 1 + 2x \quad (36b)$$

$$y_1^2 + 2y_2^2 = 6 - x \quad (36c)$$

$$y_1^3 + 2y_2^3 = 2 + x \quad (36d)$$

$$y_1^4 + 2y_2^4 = 3 + x \quad (36e)$$

$$y_1^5 + 2y_2^5 = 1 - 2x \quad (36f)$$

$$0 \leq x \leq 10 \quad (36g)$$

$$y_1^s, y_2^s \geq 0 \quad \forall s = 1, \dots, 5, \quad (36h)$$

where $\Omega = \{\omega^1, \omega^2, \omega^3, \omega^4, \omega^5\}$, with probabilities $p^1 = \frac{3}{5}, p^2 = \frac{1}{10}, p^3 = \frac{1}{20}, p^4 = \frac{3}{20}, p^5 = \frac{1}{10}$. Assume to construct a refinement chain of Ω with three levels, where scenario ω^1 is fixed across all subsets:

| | | |
|-----------|--|--|
| Level j | $\{\Omega_i^{(j)}\}_{i=1}^{m_j}$ | |
| 3 | $\Omega_1^{(3)} = \Omega$ | $(\{\omega^1, \omega^2, \omega^3, \omega^4, \omega^5\})$ |
| 2 | $(\Omega_1^{(2)}, \Omega_2^{(2)})$ | $(\{\omega^1, \omega^2, \omega^3\}, \{\omega^1, \omega^4, \omega^5\})$ |
| 1 | $(\Omega_1^{(1)}, \Omega_2^{(1)}, \Omega_3^{(1)}, \Omega_4^{(1)})$ | $(\{\omega^1, \omega^2\}, \{\omega^1, \omega^3\}, \{\omega^1, \omega^4\}, \{\omega^1, \omega^5\})$ |

Consider $\Omega_1^{(2)} = \Omega_1^{(1)} \cup \Omega_2^{(1)}$. The intra-level weights are computed as in (15) and are given by $\pi_1^{(1)} = \frac{1}{4}, \pi_2^{(1)} = \frac{1}{8}$, and $\pi_1^{(2)} = \frac{3}{8}$. Conversely, the inter-level weights are computed according to (18) and are $\pi_{1,1}^{(1,2)} = \frac{2}{3}$ and $\pi_{2,1}^{(1,2)} = \frac{1}{3}$.

The extreme points of the dual feasible regions $\Lambda_1^{(1)}$, $\Lambda_2^{(1)}$, and $\Lambda_1^{(2)}$ are as follows:

$$e_1^{(1)} = \begin{bmatrix} -\frac{6}{5} \\ -\frac{4}{5} \\ 0 \end{bmatrix} \quad e_2^{(1)} = \begin{bmatrix} -\frac{6}{5} \\ 0 \\ -\frac{4}{5} \end{bmatrix} \quad e_1^{(2)} = \begin{bmatrix} -\frac{6}{5} \\ -\frac{8}{15} \\ -\frac{4}{15} \end{bmatrix}.$$

The corresponding optimality cuts are:

$$\Omega_1^{(1)} : -6 - \frac{8}{5}x \leq \theta_1^{(1)} \quad \Omega_2^{(1)} : -\frac{14}{5} - \frac{16}{5}x \leq \theta_2^{(1)} \quad \Omega_1^{(2)} : -\frac{74}{15} - \frac{32}{15}x \leq \theta_1^{(2)}.$$

According to Proposition 4, it follows that:

$$e_1^{(2)} = \begin{bmatrix} -\frac{6}{5} \\ -\frac{8}{15} \\ -\frac{4}{15} \end{bmatrix} = \frac{2}{3} \begin{bmatrix} -\frac{6}{5} \\ -\frac{4}{5} \\ 0 \end{bmatrix} + \frac{1}{3} \begin{bmatrix} -\frac{6}{5} \\ 0 \\ -\frac{4}{5} \end{bmatrix} = \pi_{1,1}^{(1,2)} e_1^{(1)} + \pi_{1,2}^{(1,2)} e_2^{(1)}.$$

Considering the optimality cut for the problem defined over $\Omega_1^{(2)}$, Proposition 7 implies that:

$$\pi_{1,1}^{(1,2)} \left(-6 - \frac{8}{5}x \right) + \pi_{1,2}^{(1,2)} \left(-\frac{14}{5} - \frac{16}{5}x \right) = -\frac{74}{15} - \frac{32}{15}x \leq \theta_1^{(2)}.$$

With respect to the feasibility cuts, the dual feasible region Λ has a single extreme ray given by $r = 1$. Therefore, according to (8b), the five feasibility cuts corresponding to scenarios $\{\omega^1, \dots, \omega^5\}$ are respectively:

$$x \geq -\frac{1}{2} \quad x \leq 6 \quad x \geq -2 \quad x \geq -3 \quad x \leq \frac{1}{2}.$$

When considering the subset $\Omega_1^{(2)} = \{\omega^1, \omega^2, \omega^3\}$, the extreme rays of the dual feasible region $\Lambda_1^{(2)}$ are:

$$r_1 = \begin{bmatrix} -1 \\ 0 \\ 0 \end{bmatrix} \quad r_2 = \begin{bmatrix} 0 \\ -1 \\ 0 \end{bmatrix} \quad r_3 = \begin{bmatrix} 0 \\ 0 \\ -1 \end{bmatrix},$$

which is consistent with Proposition 9.

Similar results can be obtained for the other subsets of the refinement chain.

We conclude this section by establishing the main convergence result for the proposed L-shaped refinement chain cuts method, building on the theoretical developments presented thus far.

Theorem 10 *Consider a refinement chain composed by either disjoint subsets of with fixed scenarios appearing in all of them. For each level $j = 1, \dots, J$ of the refinement chain, the Benders master problem (24) at level j of the refinement chain converges to the optimal solution of the original two-stage stochastic program (3).*

Proof From Section 4.1, the classical Benders multi-cut formulation can be regarded as a special case of the proposed framework, corresponding to level 1 of the refinement chain, where all subgroups are disjoint. In the case of fixed scenarios, a lower level composed of disjoint subgroups can also be introduced. By [5], the multi-cut formulation (8) converges to the optimal solution of the original two-stage stochastic program (3).

Consider now the Benders master problem at level 2. By Proposition 8, the optimality cuts at level 2 can be decomposed as convex combinations of optimality cuts obtained at level 1, i.e., the cuts characterizing the multi-cut formulation. Moreover, Proposition 6 establishes a one-to-one correspondence between the sets of optimal dual extreme points associated with levels 1 and 2. Finally, Proposition 9 ensures that directions of unboundedness are preserved between the two levels, so that feasibility cuts are also guaranteed. Therefore, convergence of the Benders master problem at level 2 follows from convergence at level 1.

The same argument can then be applied iteratively between any two consecutive levels of the refinement chain. Hence, for each level $j = 1, \dots, J$, the Benders master problem (24) converges to the optimal solution of (3). \square

Note that the convergence result of Theorem 10 can also be established by proceeding in the opposite direction along the refinement chain. In particular, starting from the single-cut formulation at the coarsest refinement level $j = J$, the relationships established between consecutive levels can be applied recursively up to the finest level $j = 1$, yielding the same convergence result.

5 Implementation of the L-shaped refinement chain cuts method between consecutive levels

In this section, we present an algorithmic implementation of the L-shaped refinement chain cuts method between two consecutive levels $j - 1$ and j of the refinement chain. The proposed approach considers a Benders master problem defined at level j and iteratively strengthens it with feasibility and aggregated optimality cuts generated from the subproblems associated with level $j - 1$. The overall procedure is summarized in Algorithm 1.

Algorithm 1 Algorithmic implementation of the L-shaped refinement chain cuts method between consecutive levels $j - 1$ and j

Input: Two-stage stochastic program (3), refinement chain, consecutive refinement levels $j - 1$ and j , absolute tolerance ε_a , relative tolerance ε_r , time limit T_{\max}

Output: An optimal solution of the two-stage stochastic program

```

1:  $LB \leftarrow -\infty, UB \leftarrow +\infty$  ▷ Initialize lower and upper bounds
2:  $gap_a \leftarrow +\infty, gap_r \leftarrow +\infty$  ▷ Initialize absolute and relative gaps
3: while ( $gap_a > \varepsilon_a$  or  $gap_r > \varepsilon_r$ ) and CPU time  $< T_{\max}$  do
4:   Solve Benders master problem (20) at level  $j$ , with first stage solution  $\mathbf{x}^{(j)}$  and
   objective function value  $z^{(j)}$ 
5:    $LB \leftarrow \max\{LB, z^{(j)}\}$  ▷ Update the lower bound
6:    $obj_1 \leftarrow \mathbf{c}^\top \mathbf{x}^{(j)}, obj_2 \leftarrow 0$  ▷ First-stage and second-stage cost
7:   for  $k = 1, \dots, m_{j-1}$  do ▷ Loop at level  $j - 1$ 
8:     Solve dual subproblem (22)  $\mathcal{Q}_{dual}(\mathbf{x}^{(j)}, \boldsymbol{\xi}_k^{(j-1)})$  at level  $j - 1$ , with objective
     function value  $obj_k^{(j-1)}$ 
9:     if  $\mathcal{Q}_{dual}(\mathbf{x}^{(j)}, \boldsymbol{\xi}_k^{(j-1)})$  is infeasible then
10:       Obtain a dual extreme ray  $\mathbf{r}_k^{(j-1)} \in \mathcal{R}(\Lambda_k^{(j-1)})$ 
11:       Generate a feasibility cut (24b)  $(\mathbf{h}_k^{(j-1)} - \mathbf{T}_k^{(j-1)} \mathbf{x})^\top \mathbf{r}_k^{(j-1)} \leq 0$ 
12:     else
13:       Obtain a dual extreme point  $\mathbf{e}_k^{(j-1)} \in \mathcal{E}(\Lambda_k^{(j-1)})$ 
14:       Generate an optimality cut (24c)  $(\mathbf{h}_k^{(j-1)} - \mathbf{T}_k^{(j-1)} \mathbf{x})^\top \mathbf{e}_k^{(j-1)} \leq \theta_k^{(j-1)}$ 
15:     end if
16:      $obj_2 \leftarrow obj_2 + \pi_k^{(j-1)} obj_k^{(j-1)}$ 
17:   end for
18:    $UB \leftarrow \min\{UB, obj_1 + obj_2\}$  ▷ Update the upper bound
19:   Add the feasibility cuts to the Benders master problem (20) at level  $j$ 
20:   for  $i = 1, \dots, m_j$  do ▷ Loop at level  $j$ 
21:     Using (31) aggregate the optimality cuts for each  $k = 1, \dots, m_{j-1}$  such that
      $\Omega_i^{(j)} \supseteq \Omega_k^{(j-1)}$  and  $\mathcal{Q}_{dual}(\mathbf{x}^{(j)}, \boldsymbol{\xi}_k^{(j-1)})$  is feasible
22:     Add the aggregated optimality cuts to the Benders master problem (20) at
     level  $j$ 
23:   end for
24:    $gap_a \leftarrow |UB - LB|, gap_r = gap_a / |UB|$  ▷ Update the absolute and relative gap
25: end while

```

As input, we consider a two-stage stochastic program of the form (3) together with a refinement chain of probabilities based on either disjoint or fixed scenarios. As in the classical L-shaped method, the explicit enumeration of all extreme points and extreme rays of the dual feasible regions $\Lambda_i^{(j)}$, for all $i = 1, \dots, m_j$, is computationally intractable. Therefore, the proposed methodology relies on an iterative relaxation procedure. For this reason, we introduce an absolute tolerance ε_a , a relative tolerance ε_r , and a maximum CPU time limit T_{\max} as stopping criteria. At termination, provided that the time limit has not been reached, the algorithm returns a solution that is

optimal up to an absolute gap ε_a or a relative gap ε_r . To evaluate the convergence of the procedure, we iteratively update a Lower Bound (LB) and an Upper Bound (UB) on the optimal objective function value of the two-stage stochastic program. These bounds are then used to compute the absolute and relative optimality gaps that define the stopping criteria.

The algorithm starts by initializing LB and UB to $-\infty$ and $+\infty$, respectively (line 1). Similarly, the absolute and relative gaps, denoted by gap_a and gap_r , are initialized to $+\infty$ (line 2). The procedure then enters an iterative loop (lines 3–25), which constitutes the core iterative structure of the algorithm and continues until one of the stopping criteria is satisfied. At each iteration, the Benders master problem (20) defined at level j is solved, yielding a first-stage solution $\mathbf{x}^{(j)}$ and an objective function value $z^{(j)}$ (line 14). The lower bound is then updated in line 5. Subsequently, the first-stage cost is computed as $obj_1 = \mathbf{c}^\top \mathbf{x}^{(j)}$, while the second-stage cost obj_2 is initialized to zero (line 6).

The algorithm then performs two consecutive iterative procedures.

The first loop (lines 7–17) operates at refinement level $j - 1$. For each subset $\Omega_k^{(j-1)}$, with $k = 1, \dots, m_{j-1}$, the dual subproblem (22) $\mathcal{Q}_{dual}(\mathbf{x}^{(j)}, \boldsymbol{\xi}_k^{(j-1)})$ is solved, obtaining an objective function value equal to $obj_k^{(j-1)}$ (line 8). If the dual subproblem is infeasible, a dual extreme ray $\mathbf{r}_k^{(j-1)} \in \mathcal{R}(\Lambda_k^{(j-1)})$ is generated and a feasibility cut of the form (24b) is constructed (lines 9–11). Otherwise, an extreme point $\mathbf{e}_k^{(j-1)} \in \mathcal{E}(\Lambda_k^{(j-1)})$ is obtained and an optimality cut of the form (24c) is generated (lines 12–15). The second-stage contribution is then updated using the intra-level weight associated with subset $\Omega_k^{(j-1)}$ (line 16). In the infeasible case, the contribution is interpreted as $obj_k^{(j-1)} = -\infty$.

At the end of this loop, the upper bound UB is updated as shown in line 18. The generated feasibility cuts are then added to the Benders master problem at level j (line 19).

The second loop (lines 20–23) establishes the connection between optimality cuts at levels $j - 1$ and j of the refinement chain. For each subset $\Omega_i^{(j)}$, with $i = 1, \dots, m_j$, the optimality cuts generated at level $j - 1$ are aggregated using Proposition 31. More precisely, the aggregation is performed over all subsets $\Omega_k^{(j-1)}$ such that $\Omega_i^{(j)} \supseteq \Omega_k^{(j-1)}$, provided that the corresponding dual subproblem $\mathcal{Q}_{dual}(\mathbf{x}^{(j)}, \boldsymbol{\xi}_k^{(j-1)})$ is feasible. The resulting aggregated optimality cuts are then added to the Benders master problem at level j (lines 21–22).

Finally, the absolute and relative gaps are updated as reported in line 24.

Schematically, the proposed methodology is illustrated in Figure 1.

6 Numerical results

In this section, we report and discuss the numerical results of the computational experiments conducted to validate the proposed methodology. To assess the effectiveness of the L-shaped refinement chain approach, we apply it to a two-stage stochastic fixed-charge multicommodity network design problem. This class of problems commonly arises in several application domains, particularly in transportation and logistics, such

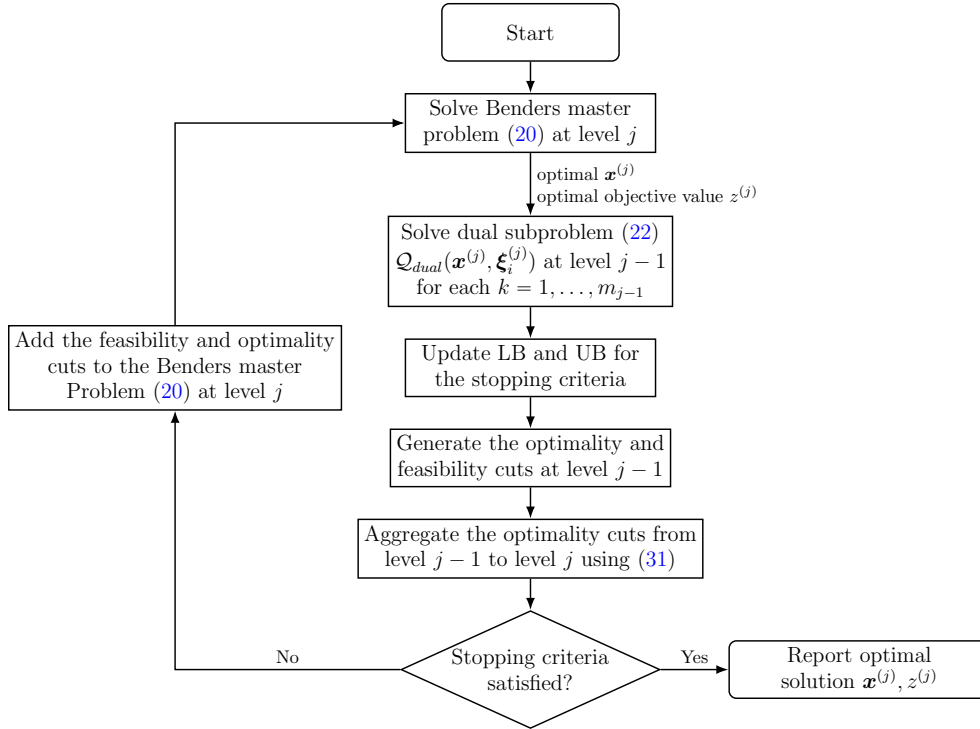


Fig. 1: Overview of the proposed L-shaped refinement chain cuts Algorithm 1

as liner shipping [14], freight and passenger rail transportation [8; 36], logistics network design [37], but also in manufacturing and telecommunications [11].

We begin in Section 6.1 by introducing the problem and describing its main characteristics, followed by its mathematical formulation in Section 6.2. Next, in Section 6.3, we derive the corresponding Benders formulations and present the details of the experimental setting considered in this study in Section 6.4. Finally, Section 6.5 reports and discusses the computational results.

6.1 Problem definition

Network design problems typically involve two sets of decisions: *design decisions*, which determine the structure and characteristics of the network, and *flow decisions*, which govern how the network is utilized for operational activities [12].

Formally, we consider a directed graph $\mathcal{G} := (\mathcal{N}, \mathcal{A})$, where \mathcal{N} and \mathcal{A} are the set of nodes and arcs, respectively, and \mathcal{K} is the set of commodities. For each node $i \in \mathcal{N}$, we define $\mathcal{N}^+(i)$ and $\mathcal{N}^-(i)$ the set of arcs emanating from i and terminating at i , respectively, i.e., $\mathcal{N}^+(i) := \{(i, j) \in \mathcal{A}\}$ and $\mathcal{N}^-(i) := \{(j, i) \in \mathcal{A}\}$. Each commodity $k \in \mathcal{K}$ needs to be transported from an origin node $on^k \in \mathcal{N}$ to a destination node $dn^k \in \mathcal{N}$.

Moreover, as in [24], we suppose that the decision-maker can externally access additional resources beyond the design network. This may occur when the total demand of the commodities exceeds the network's capacity. In such cases, external providers are employed to transport some commodities directly from their origin to destination nodes, but at a higher unit price. No capacity constraints are imposed on these direct links. Formally, let \mathcal{A}^A be the set of design arcs, i.e., the ones that are used to design the network, and \mathcal{A}^D be the set of dummy arcs associated with the commodities. Specifically, for each commodity $k \in \mathcal{K}$, set \mathcal{A}^D includes the direct arc from on^k (origin) to dn^k (destination), i.e., $\mathcal{A}^D := \{(on^k, dn^k) : \forall k \in \mathcal{K}\}$. A fixed cost $f_{ij} \in \mathbb{R}^+$ is associated with the selection of arc $(i, j) \in \mathcal{A}^A$ in the network, while $c_{ij}^k, \tilde{c}_{ij}^k \in \mathbb{R}^+$ are the costs per unit of volume of commodity $k \in \mathcal{K}$ flowed on arc $(i, j) \in \mathcal{A}^A$ and $(i, j) \in \mathcal{A}^D$, respectively.

We assume that the capacity $u_{ij} \in \mathbb{R}^+$ of each arc $(i, j) \in \mathcal{A}^A$ and the demand $d_i^k \in \mathbb{R}^+$ of commodity $k \in \mathcal{K}$ at node $i \in \mathcal{N}$ are stochastic parameters, depending on the outcome $\omega \in \Omega$ of a random experiment, i.e., $\boldsymbol{\xi}(\omega) = \{u(\omega), d(\omega)\}$. Therefore, for each $\omega \in \Omega$, possible realizations of the uncertain parameters $\{u_{ij}(\omega)\}_{(i,j) \in \mathcal{A}^A}$ and $\{d_i^k(\omega)\}_{i \in \mathcal{N}, k \in \mathcal{K}}$ occur.

The flow of each commodity $k \in \mathcal{K}$ through the network depends on its origin node on^k , its destination node dn^k and the volume to be transported. While the origin and destination nodes are known and fixed, the volume is generally uncertain [24]. Therefore, denoting by $v^k(\omega)$ the volume of commodity $k \in \mathcal{K}$ that must be transported from on^k to dn^k once the outcome $\omega \in \Omega$ is observed, the stochastic demand can be expressed as:

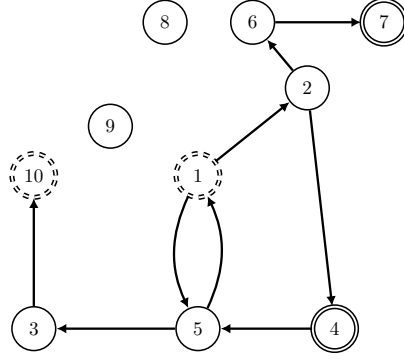
$$d_i^k(\omega) := \begin{cases} v^k(\omega) & \text{if } i = on^k \\ -v^k(\omega) & \text{if } i = dn^k \\ 0 & \text{otherwise.} \end{cases} \quad (37)$$

In terms of decision variables, let $x_{ij} \in \{0, 1\}$ be the first-stage variables associated with each arc $(i, j) \in \mathcal{A}^A$, indicating whether arc (i, j) is installed in the network. In the second stage of the problem, once the uncertainty has been revealed, the network constructed at the first stage is used to flow the commodities to meet the observed demands. Let $y_{ij}^k(\omega) \geq 0$ be the second-stage volume of commodity $k \in \mathcal{K}$ that transits through arc $(i, j) \in \mathcal{A}^A$ if the outcome $\omega \in \Omega$ is observed. Similarly for $\tilde{y}_{ij}^k(\omega) \geq 0$ for the dummy arc $(i, j) \in \mathcal{A}^D$. With respect to the previous notation, the variables x_{ij} represent the *design decisions*, while the variables $y_{ij}^k(\omega), \tilde{y}_{ij}^k(\omega)$ correspond to the *flow decisions*.

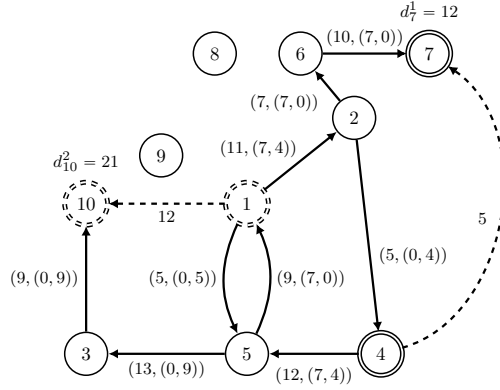
The objective is to minimize the expected total cost, which includes both the fixed costs associated with the selection of the design arcs in the first stage and the operational transportation costs incurred in the second stage for routing the commodities through the designed network and, when necessary, through the external dummy arcs. To account for risk aversion with respect to the uncertain realization of commodity demands and arc capacities, we consider a mean-risk formulation in which the second-stage cost is modeled as a convex combination of expectation and the Conditional

Value-at-Risk (CVaR) (see, e.g., [26; 51; 52]). This formulation allows the decision-maker to balance average performance and protection against high-cost realizations arising from unfavorable scenarios.

For the sake of illustration, Figure 2 reports an example of a network with two commodities, denoted by 1 and 2, which must be shipped from node 4 to node 7 and from node 1 to node 10, respectively. The left panel, Figure 2a, shows the design arcs selected in the first stage. The right panel, Figure 2b, illustrates the second-stage decisions after the realization of the uncertain demands d_7^1 and d_{10}^2 , equal to 12 and 21, respectively, as well as the realization of the arc capacities u_{ij} . At this stage, the flow decisions y_{ij}^1 and y_{ij}^2 are determined. Since the realized capacities of the design arcs are not sufficient to satisfy the demand of both commodities, the dummy arcs $(4, 7)$ and $(1, 10)$, represented by dashed lines, are activated for commodities 1 and 2, respectively. Each design arc is associated with a label of the form $(u_{ij}, (y_{ij}^1, y_{ij}^2))$, while the labels on the dummy arcs indicate the corresponding routed flows, equal to 5 and 12, respectively.



(a) First-stage decisions.



(b) Second-stage decisions.

Fig. 2: Illustrative example of a network design problem with two commodities. Origin and destination nodes associated with commodities 1 and 2 are represented by double-circle and dashed double-circle markers, respectively. Figure 2a reports the selected design arcs by solid lines. Figure 2b illustrates the second-stage flow decisions after the realization of the uncertain demands and arc capacities. The labels on the design arcs report the arc capacities u_{ij} together with the routed flows for the two commodities (y_{ij}^1, y_{ij}^2) , whereas the dashed arcs represent dummy arcs activated to satisfy the unmet demand.

6.2 Mathematical formulation

Extensively, the two-stage stochastic fixed-charge multicommodity network design problem can be formulated as follows:

$$\min_{x, y, \tilde{y}} \sum_{(i,j) \in \mathcal{A}^A} f_{ij} x_{ij} + (1 - \beta) \mathbb{E}_{\mathbb{P}} \left[\sum_{k \in \mathcal{K}} \sum_{(i,j) \in \mathcal{A}^A} c_{ij}^k y_{ij}^k(\omega) + \sum_{k \in \mathcal{K}} \sum_{(i,j) \in \mathcal{A}^D} \tilde{c}_{ij}^k \tilde{y}_{ij}^k(\omega) \right] +$$

$$+ \beta \text{CVaR}_\alpha \left[\sum_{k \in \mathcal{K}} \sum_{(i,j) \in \mathcal{A}^A} c_{ij}^k y_{ij}^k(\omega) + \sum_{k \in \mathcal{K}} \sum_{(i,j) \in \mathcal{A}^D} \tilde{c}_{ij}^k \tilde{y}_{ij}^k(\omega) \right] \quad (38a)$$

$$\text{s.t.} \quad \sum_{j \in \mathcal{N}^+(i)} \left(y_{ij}^k(\omega) + \tilde{y}_{ij}^k(\omega) \right) - \sum_{j \in \mathcal{N}^-(i)} \left(y_{ij}^k(\omega) + \tilde{y}_{ij}^k(\omega) \right) = d_i^k(\omega) \quad \forall i \in \mathcal{N}, k \in \mathcal{K}, \omega \in \Omega \quad (38b)$$

$$\sum_{k \in \mathcal{K}} y_{ij}^k(\omega) \leq u_{ij}(\omega) x_{ij} \quad \forall (i,j) \in \mathcal{A}^A, \omega \in \Omega \quad (38c)$$

$$x_{ij} \in \{0, 1\} \quad \forall (i,j) \in \mathcal{A}^A \quad (38d)$$

$$y_{ij}^k(\omega) \geq 0 \quad \forall (i,j) \in \mathcal{A}^A, k \in \mathcal{K}, \omega \in \Omega \quad (38e)$$

$$\tilde{y}_{ij}^k(\omega) \geq 0 \quad \forall (i,j) \in \mathcal{A}^D, k \in \mathcal{K}, \omega \in \Omega. \quad (38f)$$

The objective function (38a) aims to minimize the expected total cost, which consists of three components. The first term represents the fixed cost associated with the selection of the design arcs in the first stage. The second term corresponds to the expected operational cost, comprising the multicommodity flow costs over both the selected arcs and the dummy arcs, respectively. The third term accounts for the conditional value-at-risk at confidence level $\alpha \in (0, 1)$ of the same operational cost presented in the second term. The expectation and the CVaR are therefore defined consistently with respect to the same operational cost function, ensuring the coherence of the resulting mean-risk measure formulation [18]. The parameter $\beta \in [0, 1]$ controls the trade-off between the expectation and the CVaR components of the objective function. Larger values of α or β correspond to a more risk-averse decision-maker [26].

Constraints (38b) enforce flow conservation, ensuring that the demand (37) of each commodity $k \in \mathcal{K}$ is routed from its origin node on^k to its destination node dn^k . Constraints (38c) restrict the total quantity of flow that can transit through arc $(i, j) \in \mathcal{A}^A$, without violating its capacity. Finally, constraints (38d)-(38f) define the domain of the decision variables of the problem.

In the case of a discrete set of scenarios \mathcal{S} , the objective function (38a) can be expressed as a linear function [48]. Consequently, model (38) can be reformulated as the following linear program:

$$\begin{aligned} \min_{x, y, \tilde{y}, z, \tau} \quad & \sum_{(i,j) \in \mathcal{A}^A} f_{ij} x_{ij} + (1 - \beta) \sum_{s \in \mathcal{S}} p^s \left[\sum_{k \in \mathcal{K}} \sum_{(i,j) \in \mathcal{A}^A} c_{ij}^k y_{ij}^{ks} + \sum_{k \in \mathcal{K}} \sum_{(i,j) \in \mathcal{A}^D} \tilde{c}_{ij}^k \tilde{y}_{ij}^{ks} \right] + \\ & + \beta \left[\tau + \frac{1}{1 - \alpha} \sum_{s \in \mathcal{S}} p^s z^s \right] \end{aligned} \quad (39a)$$

$$\text{s.t.} \quad \sum_{j \in \mathcal{N}^+(i)} \left(y_{ij}^{ks} + \tilde{y}_{ij}^{ks} \right) - \sum_{j \in \mathcal{N}^-(i)} \left(y_{ij}^{ks} + \tilde{y}_{ij}^{ks} \right) = d_i^{ks} \quad \forall i \in \mathcal{N}, k \in \mathcal{K}, s \in \mathcal{S} \quad (39b)$$

$$\sum_{k \in \mathcal{K}} y_{ij}^{ks} \leq u_{ij}^s x_{ij} \quad \forall (i,j) \in \mathcal{A}^A, s \in \mathcal{S} \quad (39c)$$

$$\sum_{k \in \mathcal{K}} \sum_{(i,j) \in \mathcal{A}^A} c_{ij}^k y_{ij}^{ks} + \sum_{k \in \mathcal{K}} \sum_{(i,j) \in \mathcal{A}^D} \tilde{c}_{ij}^k \tilde{y}_{ij}^{ks} \leq \tau + z^s \quad \forall s \in \mathcal{S} \quad (39d)$$

$$x_{ij} \in \{0, 1\} \quad \forall (i, j) \in \mathcal{A}^A \quad (39e)$$

$$y_{ij}^{ks} \geq 0 \quad \forall (i, j) \in \mathcal{A}^A, k \in \mathcal{K}, s \in \mathcal{S} \quad (39f)$$

$$\tilde{y}_{ij}^{ks} \geq 0 \quad \forall (i, j) \in \mathcal{A}^D, k \in \mathcal{K}, s \in \mathcal{S} \quad (39g)$$

$$z^s \geq 0 \quad \forall s \in \mathcal{S} \quad (39h)$$

$$\tau \in \mathbb{R}. \quad (39i)$$

6.3 Benders formulations

In this section, we derive the Benders reformulations of model (39) corresponding to the multi-cut, single-cut, and proposed L-shaped refinement chain cuts formulations.

We begin with the multi-cut formulation. To this end, model (39) is first rewritten in the form of model (4) as follows:

$$\min_{\mathbf{x}, \tau, \theta^s} \quad \sum_{(i,j) \in \mathcal{A}^A} f_{ij} x_{ij} + \beta \tau + \sum_{s \in \mathcal{S}} p^s \theta^s \quad (40a)$$

$$\text{s.t.} \quad \mathcal{Q}(\mathbf{x}, \tau, \xi^s) \leq \theta^s \quad \forall s \in \mathcal{S} \quad (40b)$$

$$\theta^s \in \mathbb{R} \quad \forall s \in \mathcal{S} \quad (40c)$$

$$x_{ij} \in \{0, 1\} \quad \forall (i, j) \in \mathcal{A}^A \quad (40d)$$

$$\tau \in \mathbb{R}, \quad (40e)$$

where for each given scenario $s \in \mathcal{S}$ and fixed first-stage variables $\mathbf{x} \in \{0, 1\}^{|\mathcal{A}^A|}$ and $\tau \in \mathbb{R}$, the second-stage problem is defined as:

$$\mathcal{Q}(\mathbf{x}, \tau, \xi^s) := \min_{\mathbf{y}, \tilde{\mathbf{y}}^s, z^s} (1 - \beta) \left[\sum_{k \in \mathcal{K}} \sum_{(i,j) \in \mathcal{A}^A} c_{ij}^k y_{ij}^{ks} + \sum_{k \in \mathcal{K}} \sum_{(i,j) \in \mathcal{A}^D} \tilde{c}_{ij}^k \tilde{y}_{ij}^{ks} \right] + \frac{\beta}{1 - \alpha} z^s \quad (41a)$$

$$\text{s.t.} \quad \sum_{j \in \mathcal{N}^+(i)} (y_{ij}^{ks} + \tilde{y}_{ij}^{ks}) - \sum_{j \in \mathcal{N}^-(i)} (y_{ij}^{ks} + \tilde{y}_{ij}^{ks}) = d_i^{ks} \quad \forall i \in \mathcal{N}, k \in \mathcal{K} \quad (41b)$$

$$\sum_{k \in \mathcal{K}} y_{ij}^{ks} \leq u_{ij}^s x_{ij} \quad \forall (i, j) \in \mathcal{A}^A \quad (41c)$$

$$\sum_{k \in \mathcal{K}} \sum_{(i,j) \in \mathcal{A}^A} c_{ij}^k y_{ij}^{ks} + \sum_{k \in \mathcal{K}} \sum_{(i,j) \in \mathcal{A}^D} \tilde{c}_{ij}^k \tilde{y}_{ij}^{ks} \leq \tau + z^s \quad (41d)$$

$$y_{ij}^{ks} \geq 0 \quad \forall (i, j) \in \mathcal{A}^A, k \in \mathcal{K} \quad (41e)$$

$$\tilde{y}_{ij}^{ks} \geq 0 \quad \forall (i, j) \in \mathcal{A}^D, k \in \mathcal{K} \quad (41f)$$

$$z^s \geq 0. \quad (41g)$$

By taking into account (37), the dual of subproblem (41) is as follows:

$$\mathcal{Q}_{dual}(\mathbf{x}, \tau, \xi^s) := \max_{\lambda^s, \mu^s, \gamma^s} \sum_{k \in \mathcal{K}} v^{ks} (\lambda_{on^k}^{ks} - \lambda_{dn^k}^{ks}) - \sum_{(i,j) \in \mathcal{A}^A} u_{ij}^s x_{ij} \mu_{ij}^s - \tau \gamma^s \quad (42a)$$

$$\text{s.t. } \lambda_i^{ks} - \lambda_j^{ks} - \mu_{ij}^s - c_{ij}^k \gamma^s \leq (1 - \beta)c_{ij}^k \quad \forall (i, j) \in \mathcal{A}^A, k \in \mathcal{K} \quad (42b)$$

$$\lambda_i^{ks} - \lambda_j^{ks} - \tilde{c}_{ij}^k \gamma^s \leq (1 - \beta)\tilde{c}_{ij}^k \quad \forall (i, j) \in \mathcal{A}^D, k \in \mathcal{K} \quad (42c)$$

$$(1 - \alpha)\gamma^s \leq \beta \quad (42d)$$

$$\lambda_i^{ks} \in \mathbb{R} \quad \forall i \in \mathcal{N}, k \in \mathcal{K} \quad (42e)$$

$$\mu_{ij}^s \geq 0 \quad \forall (i, j) \in \mathcal{A}^A \quad (42f)$$

$$\gamma^s \geq 0. \quad (42g)$$

Note that in the current setting, model (38) is always feasible due to the availability of recourse actions on the set of dummy arcs. As a result, subproblem (41) is always feasible too, and only Benders optimality cuts need to be generated. Given a first-stage solution (\mathbf{x}, τ) and, for each scenario $s \in \mathcal{S}$, a dual solution $(\boldsymbol{\lambda}^s, \boldsymbol{\mu}^s, \gamma^s)$ of subproblem $\mathcal{Q}_{\text{dual}}(\mathbf{x}, \tau, \xi^s)$, the optimality cut to be added to the master problem (40) takes the following form:

$$\sum_{k \in \mathcal{K}} v^{ks} (\lambda_{on^k}^{ks} - \lambda_{dn^k}^{ks}) - \sum_{(i,j) \in \mathcal{A}^A} u_{ij}^s x_{ij} \mu_{ij}^s - \tau \gamma^s \leq \theta^s \quad \forall s \in \mathcal{S}. \quad (43)$$

In the case of single-cut formulation (9), all variables θ^s are aggregated into a single variable Θ . This leads to the following master problem:

$$\min_{\mathbf{x}, \tau, \Theta} \sum_{(i,j) \in \mathcal{A}^A} f_{ij} x_{ij} + \beta \tau + \Theta \quad (44a)$$

$$\text{s.t. } \sum_{s \in \mathcal{S}} \sum_{k \in \mathcal{K}} p^s v^{ks} (\lambda_{on^k}^{ks} - \lambda_{dn^k}^{ks}) - \sum_{s \in \mathcal{S}} \sum_{(i,j) \in \mathcal{A}^A} p^s u_{ij}^s x_{ij} \mu_{ij}^s - \tau \sum_{s \in \mathcal{S}} p^s \gamma^s \leq \Theta \quad (44b)$$

$$\Theta \in \mathbb{R} \quad (44c)$$

$$x_{ij} \in \{0, 1\} \quad \forall (i, j) \in \mathcal{A}^A \quad (44d)$$

$$\tau \in \mathbb{R}. \quad (44e)$$

Constraint (44b) represents the single-cut version of the optimality cut given in (43), where $(\boldsymbol{\lambda}^s, \boldsymbol{\mu}^s, \gamma^s)$ are solutions of subproblem (42) for each scenario $s \in \mathcal{S}$.

Consider now a refinement chain of the scenario set \mathcal{S} , composed either of disjoint subgroups or of subgroups with fixed scenarios. Fix a level $j \in \{1, \dots, J\}$ of the refinement chain. The Benders master problem (24) at level j is given by:

$$\min_{\mathbf{x}, \tau, \theta_i^{(j)}} \sum_{(i,j) \in \mathcal{A}^A} f_{ij} x_{ij} + \beta \tau + \sum_{i=1}^{m_j} \pi_i^{(j)} \theta_i^{(j)} \quad (45a)$$

$$\text{s.t. } \mathcal{Q}(\mathbf{x}, \tau, \xi_i^{(j)}) \leq \theta_i^{(j)} \quad \forall i = 1, \dots, m_j \quad (45b)$$

$$\theta_i^{(j)} \in \mathbb{R} \quad \forall i = 1, \dots, m_j \quad (45c)$$

$$x_{ij} \in \{0, 1\} \quad \forall (i, j) \in \mathcal{A}^A \quad (45d)$$

$$\tau \in \mathbb{R}. \quad (45e)$$

For fixed first-stage variables \mathbf{x} and τ , the recourse function $\mathcal{Q}(\mathbf{x}, \tau, \xi_i^{(j)})$, defined as in (21), is obtained by minimizing:

$$\sum_{s: \omega^s \in \Omega_i^{(j)}} p_{\Omega_i^{(j)}}^s \left\{ (1 - \beta) \left[\sum_{k \in \mathcal{K}} \sum_{(i,j) \in \mathcal{A}^A} c_{ij}^k y_{ij}^{ks} + \sum_{k \in \mathcal{K}} \sum_{(i,j) \in \mathcal{A}^D} \tilde{c}_{ij}^k \tilde{y}_{ij}^{ks} \right] + \frac{\beta}{1 - \alpha} z^s \right\},$$

with respect to the second-stage decision variables \mathbf{y}^s , $\tilde{\mathbf{y}}^s$, and z^s , for all scenarios $s \in \mathcal{S}$ such that $\omega^s \in \Omega_i^{(j)}$. The constraints of the corresponding recourse problem are those in (41b)–(41g), replicated for all scenarios belonging to the subgroup $\Omega_i^{(j)}$.

Therefore, as in (22), the dual recourse problem associated with subgroup $\Omega_i^{(j)}$ is given by:

$$\max_{\lambda^s, \mu^s, \gamma^s: \omega^s \in \Omega_i^{(j)}} \sum_{s: \omega^s \in \Omega_i^{(j)}} \left[\sum_{k \in \mathcal{K}} v^{ks} (\lambda_{on^k}^{ks} - \lambda_{dn^k}^{ks}) - \sum_{(i,j) \in \mathcal{A}^A} u_{ij}^s x_{ij} \mu_{ij}^s - \tau \gamma^s \right] \quad (46a)$$

$$\text{s.t. } \lambda_i^{ks} - \lambda_j^{ks} - \mu_{ij}^s - c_{ij}^k \gamma^s \leq p_{\Omega_i^{(j)}}^s (1 - \beta) c_{ij}^k \quad \forall (i, j) \in \mathcal{A}^A, k \in \mathcal{K}, s: \omega^s \in \Omega_i^{(j)} \quad (46b)$$

$$\lambda_i^{ks} - \lambda_j^{ks} - \tilde{c}_{ij}^k \gamma^s \leq p_{\Omega_i^{(j)}}^s (1 - \beta) \tilde{c}_{ij}^k \quad \forall (i, j) \in \mathcal{A}^D, k \in \mathcal{K}, \forall s: \omega^s \in \Omega_i^{(j)} \quad (46c)$$

$$(1 - \alpha) \gamma^s \leq p_{\Omega_i^{(j)}}^s \beta \quad \forall s: \omega^s \in \Omega_i^{(j)} \quad (46d)$$

$$\lambda_i^{ks} \in \mathbb{R} \quad \forall i \in \mathcal{N}, k \in \mathcal{K}, s: \omega^s \in \Omega_i^{(j)} \quad (46e)$$

$$\mu_{ij}^s \geq 0 \quad \forall (i, j) \in \mathcal{A}^A, s: \omega^s \in \Omega_i^{(j)} \quad (46f)$$

$$\gamma^s \geq 0 \quad \forall s: \omega^s \in \Omega_i^{(j)}. \quad (46g)$$

The optimal solutions of (46) are then used to generate the optimality cuts (24c), which are added to the Benders master problem at level j , given in (45).

6.4 Experimental setting

We tested the proposed L-shaped refinement chain cuts method on a selection of benchmark instances from the multicommodity network design literature. In particular, we considered the Canad R-instances introduced in [9] and publicly available at <https://commalab.di.unipi.it/datasets/mmcf/#Canad>. With respect to the network structure, we considered three classes of instances: R04 (small), R05 (medium), and R07 (large). The main characteristics of these instances are summarized in Table 1.

The scenarios associated with uncertain arc capacities and commodity demands were generated according to the methodology proposed in [22]. For all the instances, we considered scenario trees composed of 256 scenarios.

Table 1: Canad R-instances considered in the computational experiments.

| Name | Size | Nodes $ \mathcal{N} $ | Arcs $ \mathcal{A} $ | Commodities $ \mathcal{K} $ |
|------|--------|-----------------------|----------------------|-----------------------------|
| R04 | small | 10 | 60 | 10 |
| R05 | medium | 10 | 60 | 25 |
| R07 | large | 10 | 82 | 10 |

In the construction of the refinement chain, we considered three different approaches. The first approach is based on a disjoint sequential partition, in which scenarios are grouped sequentially (e.g., for pairs of scenarios, groups are composed of scenarios 1–2, 3–4, and so on). The second and third approaches are based on the optimal grouping methodology proposed in [35]. In this case, we considered both disjoint partitions and fixed-scenario groupings, where each group is constructed with a fixed reference scenario, identified by the optimal grouping procedure itself.

Regarding the parameters of the objective function, we considered $\beta = 0.5$, i.e., mean-risk formulation with equal weights assigned to expectation and CVaR, and $\alpha = 0.95$ as the confidence level of the CVaR. For the small and medium instances, we imposed a time limit of $T_{\max} = 86400\text{s}$ (24 hours). For the large instance R07, preliminary experiments showed that neither the multi-cut method, the single-cut method, nor the proposed refinement chain cuts method were able to reach optimality within this limit. Therefore, we reduced the time limit to 10800s (3 hours) and focused the analysis on the quality of the incumbent solutions. In Algorithm 1, the absolute and relative tolerances were set to $\varepsilon_a = \varepsilon_r = 10^{-6}$.

Both the implementation for a fixed refinement level and Algorithm 1 between consecutive refinement levels were developed in Python 3.12.2 using Gurobi Optimizer v13.0.1 with a MIPGap equal to 10^{-5} . All experiments were performed on the Galileo100 HPC cluster at CINECA using 1 node, 8 CPUs per task, and 64 GB of RAM.

6.5 Results and discussion

Tables 2 and 3 analyze the performance obtained when solving model (24) at a fixed refinement level. For the R04 instance, all refinement levels yield significant reductions with respect to the single-cut formulation, with the largest improvement obtained by the optimal disjoint grouping with group size 2, corresponding to a reduction of 98.51%. Interestingly, this configuration also outperforms the multi-cut formulation, indicating that a limited degree of scenario aggregation can provide a better balance between the number of cuts generated and the complexity of the master problem. A similar behavior is observed for the R05 instance, where the best performance is achieved by the fixed-scenario optimal grouping with group size 16, yielding a reduction of 68.59%.

The results for the larger R07 instance confirm the trends observed for the R04 and R05 instances. Since all runs reached the prescribed time limit, performance is assessed in terms of the final relative optimality gap. This gap is computed as in line

24 of Algorithm 1, where the lower bound (LB) and upper bound (UB) are evaluated for the corresponding fixed level of the refinement chain. The best result is obtained with group size 2, which reduces the final gap by 65.78% with respect to the single-cut formulation. More generally, all aggregation levels up to group size 32 produce substantial gap reductions, whereas coarser aggregations (group sizes 64 and 128) deteriorate performance and even become worse than the single-cut formulation. This behavior suggests that excessive scenario aggregation weakens the approximation of the recourse function, leading to slower convergence of the Benders algorithm.

A comparison between sequential and optimal grouping strategies reveals that the benefits of optimization-driven partitions are strongly instance dependent. For the R04 instance, the optimal grouping strategy provides the best performance at group sizes 2 and 128, yielding the largest time reductions among all tested configurations. It also outperforms sequential grouping at group size 8, although the improvement is less pronounced. For the R05 instance, optimal grouping is particularly effective for intermediate aggregation levels and provides the best results for group sizes 4, 16, and 32. However, the superiority of optimal grouping is not systematic, as sequential grouping remains competitive and occasionally superior for other aggregation levels. These observations indicate that the effectiveness of a partition depends on the interplay between the scenario structure, the aggregation scheme, and the resulting strength of the generated Benders cuts.

Tables 4 and 5 evaluate the iterative refinement procedure proposed in Algorithm 1, where information generated at one refinement level is transferred to the next level through the inter-level cut relationship. For the R04 instance, Algorithm 1 is particularly effective when moving between the finest refinement levels. The best result is obtained for the transition from group size 1 to group size 2, achieving a reduction of 98.61% relative to the single-cut formulation, which improves upon the corresponding fixed-level approach. Similar behavior is observed for the transition from group size 2 to group size 4. As the refinement levels become coarser, the computational advantage progressively decreases.

For the R05 instance, the gains obtained through the iterative procedure are more moderate. The best performance is observed for the transition between levels 16 and 32, with a reduction of 62.28%. Although Algorithm 1 remains competitive, the improvements are generally smaller than those observed for R04.

Finally, the results for the R07 instance further highlight the importance of transferring information between consecutive refinement levels. The transitions from group size 1 to 2 and from 2 to 4 achieve the largest gap reductions, namely 61.44% and 53.51%, respectively. In contrast, transitions involving coarser aggregation levels lead to a deterioration in solution quality, with negative reductions observed for the largest group sizes. This behavior indicates that the Benders cuts inherited from one refinement level provide increasingly less informative approximations of the recourse function when transferred to refinement levels characterized by a significantly larger number of scenario groups.

To further investigate the behavior of Algorithm 1 when solving the large-scale R07 instance, Figure 3 reports the logarithm of the relative gap as a function of the number of Benders iterations. The figure compares the classical multi-cut and

Table 2: Detailed results for the R04 and R05 instances with 256 scenarios and $\beta = 0.5$, obtained by solving model (24) at different levels of the refinement chain. The time reduction is computed with respect to the single-cut formulation. For each instance, the best reduction is reported in bold, while results that also outperform the multi-cut formulation are underlined.

| Instance | Disjoint partitions | | | | | | Fixed-scenario | | | |
|----------|---------------------|---------------|---------------------|---------------|------------------|----------------------|------------------|---------------|------------------|----------------------|
| | Group size | No. of groups | Sequential grouping | | Optimal grouping | | Group size | No. of groups | Optimal grouping | |
| | | | Time (s) | Time red. (%) | Time (s) | Time red. (%) | | | Time (s) | Time red. (%) |
| R04 | 1 (multi-cut) | 256 | 876.38 | 97.41% | 876.38 | 97.41% | — | — | — | — |
| | 2 | 128 | 1005.75 | 97.03% | 505.35 | <u>98.51%</u> | 2 | 255 | 1135.79 | 96.65% |
| | 4 | 64 | 904.86 | 97.33% | 1759.61 | 94.81% | 4 | 85 | 1053.57 | 96.89% |
| | 8 | 32 | 1554.00 | 95.41% | 1414.93 | 95.82% | — | — | — | — |
| | 16 | 16 | 3480.50 | 89.73% | 3700.02 | 89.08% | 16 | 17 | 1690.47 | 95.01% |
| | 32 | 8 | 3832.67 | 88.69% | 4209.92 | 87.57% | — | — | — | — |
| | 64 | 4 | 15427.53 | 54.46% | 31593.89 | 6.75% | — | — | — | — |
| | 128 | 2 | 19290.63 | 43.06% | 15035.36 | 55.62% | — | — | — | — |
| | 256 (single-cut) | 1 | 33880.20 | 0.00% | 33880.20 | 0.00% | 256 (single-cut) | 1 | 33880.20 | 0.00% |
| R05 | 1 (multi-cut) | 256 | 3268.19 | 68.02% | 3268.19 | 68.02% | — | — | — | — |
| | 2 | 128 | 4677.10 | 53.36% | 5597.87 | 45.23% | 2 | 255 | 5060.38 | 50.49% |
| | 4 | 64 | 5687.08 | 44.35% | 3727.93 | 63.52% | 4 | 85 | 3276.99 | 67.94% |
| | 8 | 32 | 3864.34 | 62.19% | 9010.64 | 11.83% | — | — | — | — |
| | 16 | 16 | 5243.62 | 48.69% | 3453.01 | 66.21% | 16 | 17 | 3210.15 | <u>68.59%</u> |
| | 32 | 8 | 3807.63 | 62.74% | 3232.68 | <u>68.37%</u> | — | — | — | — |
| | 64 | 4 | 4141.67 | 59.48% | 5695.52 | 44.27% | — | — | — | — |
| | 128 | 2 | 7899.18 | 22.71% | 8286.60 | 18.92% | — | — | — | — |
| | 256 (single-cut) | 1 | 10220.09 | 0.00% | 10220.09 | 0.00% | 256 (single-cut) | 1 | 10220.09 | 0.00% |

Table 3: Detailed results for the R07 instance with 256 scenarios and $\beta = 0.5$, obtained by solving model (24) at different levels of the refinement chain. The relative gap reduction is computed with respect to the single-cut formulation. The best reduction is reported in bold, while results that also outperform the multi-cut formulation are underlined.

| Instance | Disjoint partitions | | | | Fixed-scenario | | | |
|----------|---------------------|---------------|-----------------------|-----------------------|----------------|---------------|-----------------------|-----------------------|
| | Group size | No. of groups | Optimal grouping | | Group size | No. of groups | Optimal grouping | |
| | | | Relative gap | Relative gap red. (%) | | | Relative gap | Relative gap red. (%) |
| R07 | 1 | 256 | 1.81×10^{-2} | 28.16% | — | — | — | — |
| | 2 | 128 | 8.60×10^{-3} | 65.78% | 2 | 255 | 1.50×10^{-2} | <u>40.25%</u> |
| | 4 | 64 | 1.14×10^{-2} | <u>54.50%</u> | 4 | 85 | 1.42×10^{-2} | <u>43.56%</u> |
| | 8 | 32 | 1.42×10^{-2} | <u>43.62%</u> | — | — | — | — |
| | 16 | 16 | 1.47×10^{-2} | <u>41.70%</u> | 16 | 17 | 1.66×10^{-2} | <u>33.89%</u> |
| | 32 | 8 | 1.79×10^{-2} | <u>28.87%</u> | — | — | — | — |
| | 64 | 4 | 2.74×10^{-2} | -9.13% | — | — | — | — |
| | 128 | 2 | 2.70×10^{-2} | -7.21% | — | — | — | — |
| | 256 | 1 | 2.51×10^{-2} | 0.00% | 256 | 1 | 2.51×10^{-2} | 0.00% |

Table 4: Detailed results for the R04 and R05 instances with 256 scenarios and $\beta = 0.5$, obtained by applying Algorithm 1 between consecutive levels of the refinement chain. The time reduction is computed with respect to the single-cut formulation. For each instance, the best reduction is reported in bold, while results that also outperform the multi-cut formulation are underlined.

| Instance | Consecutive levels | Disjoint partitions | | | |
|----------|--------------------|---------------------|----------------------|------------------|---------------|
| | | Sequential grouping | | Optimal grouping | |
| | | Time (s) | Time red. (%) | Time (s) | Time red. (%) |
| R04 | 1-2 | 470.83 | <u>98.61%</u> | 645.71 | <u>98.09%</u> |
| | 2-4 | 843.95 | <u>97.51%</u> | 1993.86 | <u>94.11%</u> |
| | 4-8 | 2264.57 | 93.32% | 3446.07 | 89.83% |
| | 8-16 | 2762.38 | 91.85% | 3947.77 | 88.35% |
| | 16-32 | 12356.87 | 63.53% | 4502.34 | 86.71% |
| | 32-64 | 5509.98 | 83.74% | 24865.04 | 26.61% |
| | 64-128 | 15189.61 | 55.17% | 29964.42 | 11.56% |
| | 128-256 | 14792.84 | 56.34% | 48151.83 | 1.33% |
| R05 | 1-2 | 7991.12 | 21.81% | 7833.45 | 23.35% |
| | 2-4 | 6193.63 | 39.40% | 26194.87 | -156.31% |
| | 4-8 | 4242.10 | 58.49% | 10108.77 | 1.09% |
| | 8-16 | 4676.97 | 54.24% | 5595.39 | 45.25% |
| | 16-32 | 3854.77 | 62.28% | 6720.51 | 34.24% |
| | 32-64 | 7484.40 | 26.77% | 11073.77 | -8.35% |
| | 64-128 | 7654.11 | 25.11% | 10247.13 | -0.26% |
| | 128-256 | 7419.94 | 27.40% | 8230.61 | 19.47% |

Table 5: Detailed results for the R07 instance with 256 scenarios and $\beta = 0.5$, obtained by applying Algorithm 1 between consecutive levels of the refinement chain. The relative gap reduction is computed with respect to the single-cut formulation. The best reduction is reported in bold, while results that also outperform the multi-cut formulation are underlined.

| Instance | Consecutive levels | Disjoint partitions | |
|----------|--------------------|-----------------------|-----------------------|
| | | Optimal grouping | |
| | | Relative gap | Relative gap red. (%) |
| R07 | 1-2 | 9.69×10^{-3} | <u>61.44%</u> |
| | 2-4 | 1.17×10^{-2} | <u>53.51%</u> |
| | 4-8 | 2.13×10^{-2} | 15.35% |
| | 8-16 | 1.65×10^{-2} | <u>34.40%</u> |
| | 16-32 | 2.51×10^{-2} | 0.24% |
| | 32-64 | 3.53×10^{-2} | -40.38% |
| | 64-128 | 6.99×10^{-2} | -178.14% |
| | 128-256 | 2.55×10^{-2} | -1.47% |

single-cut formulations with Algorithm 1 applied to different pairs of consecutive levels of the refinement chain, from group sizes 1–2 up to group sizes 16–32. To improve readability, markers are displayed every 10 iterations for the multi-cut formulation and for the algorithm applied between group sizes 1 and 2, and every 25 iterations for the remaining curves.

First, we note that the number of iterations completed within the three-hour time limit reflects the different sizes of the corresponding master problems. The single-cut formulation performs 851 iterations, whereas the multi-cut formulation completes only 73 iterations. The refinement-based algorithm lies between these two extremes, with the number of iterations depending on the pair of refinement levels considered; for example, the transition between group sizes 1 and 2 completes 108 iterations. This behavior is explained by the number of optimality cuts added at each iteration. The multi-cut formulation generates one cut for each scenario, leading to a significantly larger master problem and consequently longer solution times per iteration. At the opposite extreme, the single-cut formulation adds only one cut per iteration, resulting in much faster master problem solution times and therefore a substantially larger number of iterations.

Second, the single-cut formulation consistently exhibits the slowest convergence rate, maintaining the largest relative gap throughout the entire solution process. This confirms the weaker approximation of the recourse function provided by a highly aggregated representation of the scenario set.

Finally, the comparison between the multi-cut formulation and Algorithm 1 highlights an interesting trade-off. During the initial phase of the solution process, up to approximately iteration 57, the multi-cut formulation achieves lower relative gaps than the proposed algorithm between group sizes 1–2, indicating that the larger number of cuts generated at each iteration provides a stronger approximation of the recourse function. However, after this point the proposed algorithm overtakes the multi-cut formulation and achieves smaller relative gaps. This behavior suggests that the refinement chain strategy is able to preserve much of the strength of the multi-cut approach while maintaining a significantly smaller master problem, ultimately leading to better overall convergence within the available computational time.

Overall, the computational study highlights the existence of an intermediate region of the refinement chain that provides the most favorable trade-off between the strength of the generated cuts and the complexity of the master problem. The proposed refinement chain cuts framework successfully generalizes both single-cut and multi-cut formulations, while offering additional flexibility to identify aggregation levels that can significantly improve computational performance. A particularly relevant observation is that the best-performing configurations are consistently found near the multi-cut level of the refinement chain, typically for group sizes between 2 and 32 scenarios. In contrast, coarser aggregation levels and, in particular, the single-cut formulation generally lead to inferior performance. This finding suggests that a limited amount of scenario aggregation is often sufficient to reduce the burden associated with managing a large number of cuts while preserving a strong approximation of the recourse function. Furthermore, the iterative refinement procedure outlined in Algorithm 1 proves particularly effective when applied between finely spaced refinement levels.

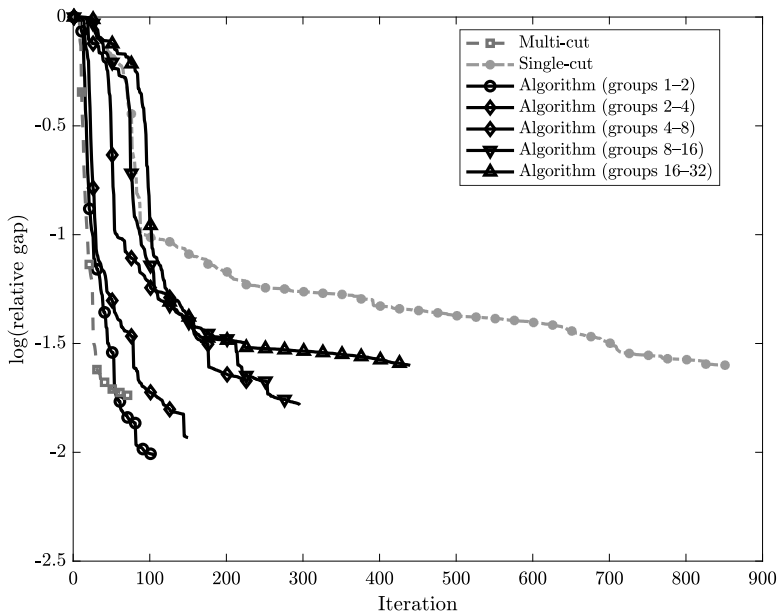


Fig. 3: Logarithm of the relative gap as a function of the number of Benders iterations for the R07 instance. Comparison between the multi-cut formulation, the single-cut formulation, and the refinement-based Algorithm 1 applied between consecutive levels of the refinement chain.

7 Conclusions

In this paper, we introduced a novel *L-shaped refinement chain cuts method* for solving two-stage stochastic programs by integrating the refinement chain of scenarios within the classical L-shaped decomposition framework. We proposed a generalized decomposition approach in which one subproblem is solved for each subgroup of scenarios at every refinement level, thereby encompassing both the classical multi-cut and single-cut L-shaped methods as special cases. We also established theoretical convergence properties for every level of the refinement chain and characterized the relationships between consecutive refinement levels in terms of feasibility and optimality cuts. These results enabled the development of an iterative refinement-based solution algorithm capable of exploiting information generated across different levels of the refinement chain. Finally, we demonstrated the effectiveness of the proposed framework on a two-stage stochastic fixed-charge multicommodity network design problem under a mean-risk formulation, showing competitive computational performance and highlighting the applicability of the proposed approach to large-scale risk-averse stochastic optimization problems.

Building on these results, there are several promising directions for future research, both from methodological and computational perspectives. First, the proposed framework could be extended to multi-stage stochastic programming problems in a nested Benders decomposition fashion. Such an extension would allow the refinement chain structure to be exploited across multiple stages of the stochastic process. Second, alternative approaches for constructing the refinement chain of scenarios could be investigated and integrated within the proposed decomposition framework. This would provide greater flexibility in the definition of scenario subgroups and could potentially improve computational tractability.

From a computational perspective, third, advanced refinement-based strategies across multiple levels of the refinement chain could be developed, allowing the derivation of an algorithm that adaptively refines and explores selected subsets of scenarios in greater detail. This could further enhance both the efficiency and the convergence behavior of the proposed framework. Fourth, the development of strategies capable of identifying *a priori* the most promising aggregation level and scenario grouping strategy represents an interesting research direction. The computational results suggest that the best performance is often achieved at intermediate levels of the refinement chain and that the effectiveness of a given partition is strongly instance dependent. Therefore, deriving indicators or learning-based approaches able to predict suitable aggregation structures before the optimization process could significantly improve the practical applicability of the proposed framework. Finally, acceleration and stabilization techniques for Benders decomposition, such as those proposed in [43; 59], could be incorporated to further improve the computational performance of the proposed method. The integration of such techniques could significantly reduce the number of iterations and improve the convergence of the algorithm on large-scale instances.

References

- [1] Bertsimas, D., Cory-Wright, R., Pauphilet, J., Petridis, P.: A stochastic benders decomposition scheme for large-scale stochastic network design. *INFORMS J. Comput.* **37**(5), 1163–1181 (2025)
- [2] Benders, J.F.: Partitioning procedures for solving mixed-variables programming problems. *Numer. Math.* **4**(1), 238–252 (1962)
- [3] Belieres, S., Hewitt, M.: Hedging against uncertainty in transportation network design through flexible scheduling. *Omega* **126**, 103045 (2024)
- [4] Belieres, S., Hewitt, M.: Stochastic scheduled service network design problem with flexible schedules: Mathematical formulations and benders decomposition-based solution approach. *Ann. Oper. Res.*, 1–25 (2026)
- [5] Birge, J.R., Louveaux, F.V.: A multicut algorithm for two-stage stochastic linear programs. *Eur. J. Oper. Res.* **34**(3), 384–392 (1988)
- [6] Birge, J.R., Louveaux, F.: *Introduction to Stochastic Programming*. Springer,

New York (2011)

- [7] Bayraksan, G., Maggioni, F., Faccini, D., Yang, M.: Bounds for multistage mixed-integer distributionally robust optimization. *SIAM J. Optim.* **34**(1), 682–717 (2024)
- [8] Chouman, M., Crainic, T.G.: In: Crainic, T.G., Gendreau, M., Gendron, B. (eds.) *Freight Railroad Service Network Design*, pp. 383–426. Springer, Cham (2021)
- [9] Crainic, T.G., Frangioni, A., Gendron, B.: Bundle-based relaxation methods for multicommodity capacitated fixed charge network design. *Discret. Appl. Math.* **112**(1), 73–99 (2001). *Combinatorial Optimization Symposium, Selected Papers*
- [10] Cavaliere, F., Fischetti, M., Roberti, R., Salvagnin, D.: Models and algorithms for the time window assignment traveling salesperson problem with stochastic travel times. *Eur. J. Oper. Res.* **329**(1), 96–111 (2026)
- [11] Crainic, T.G., Gendron, B., Akhavan Kazemzadeh, M.R.: A taxonomy of multilayer network design and a survey of transportation and telecommunication applications. *Eur. J. Oper. Res.* **303**(1), 1–13 (2022)
- [12] Crainic, T.G., Gendreau, M., Gendron, B. (eds.): *Network Design with Applications to Transportation and Logistics*. Springer, Cham (2021)
- [13] Crainic, T.G., Hewitt, M., Maggioni, F., Rei, W.: Partial benders decomposition: General methodology and application to stochastic network design. *Transp. Sci.* **55**(2), 414–435 (2021)
- [14] Christiansen, M., Hellsten, E., Pisinger, D., Sacramento, D., Vilhelmsen, C.: Liner shipping network design. *Eur. J. Oper. Res.* **286**(1), 1–20 (2020)
- [15] Cordeau, J.-F., Klibi, W., Nickel, S.: In: Crainic, T.G., Gendreau, M., Gendron, B. (eds.) *Logistics Network Design*, pp. 599–625. Springer, Cham (2021)
- [16] Cavagnini, R., Maggioni, F., Bertazzi, L., Hewitt, M.: A two-stage stochastic programming model for bike-sharing systems with rebalancing. *EURO J. Transp. Logist.* **13**, 100140 (2024)
- [17] Dupačová, J., Consigli, G., Wallace, S.W.: Scenarios for multistage stochastic programs. *Ann. Oper. Res.* **100**, 25–53 (2000)
- [18] Dentcheva, D., Ruszczyński, A.P.: *Risk-averse Optimization and Control*. Springer, Cham (2024)
- [19] Frauendorfer, K., Kuhn, D., Schürle, M.: In: Infanger, G. (ed.) *Barycentric Bounds in Stochastic Programming: Theory and Application*, pp. 67–96. Springer, New York, NY (2011)

- [20] Geoffrion, A.M.: Elements of large scale mathematical programming part ii: Synthesis of algorithms and bibliography. *Manage. Sci.* **16**(11), 676–691 (1970)
- [21] Geoffrion, A.M.: Elements of large-scale mathematical programming part i: Concepts. *Manage. Sci.* **16**(11), 652–675 (1970)
- [22] Høyland, K., Kaut, M., Wallace, S.W.: A heuristic for moment-matching scenario generation. *Comput. Optim. Appl.* **24**(2), 169–185 (2003)
- [23] Hewitt, M., Ortmann, J., Rei, W.: Decision-based scenario clustering for decision-making under uncertainty. *Ann. Oper. Res.* **315**(2), 747–771 (2022)
- [24] Hewitt, M., Rei, W., Wallace, S.W.: In: Crainic, T.G., Gendreau, M., Gendron, B. (eds.) *Stochastic Network Design*, pp. 283–315. Springer, Cham (2021)
- [25] Hosseini, M., Turner, J.: Deepest cuts for benders decomposition. *Oper. Res.* **73**(5), 2591–2609 (2025)
- [26] Mahmutogullari, A., Çavuş, O., Aktürk, M.S.: Bounds on risk-averse mixed-integer multi-stage stochastic programming problems with mean-cvar. *Eur. J. Oper. Res.* **266**(2), 595–608 (2018)
- [27] Jaoui, N., Klibi, W., El Hachemi, N., Aouam, T., Fender, M.: Multi-cycle production network design under supply uncertainty. *Eur. J. Oper. Res.* **330**(3), 816–837 (2026)
- [28] Kaltis, T., Saharidis, G.K.D.: Literature review on benders cut selection and a multiple cut generation scheme. *INFOR: Inf. Syst. Oper. Res.*, 1–27 (2025)
- [29] Kuhn, D.: In: Beckmann, M., Künzi, H.P., Fandel, G., Trockel, W., Basile, A., Drexl, A., Dawid, H., Inderfurth, K., Kürsten, W., Schittko, U. (eds.) *Barycentric approximation scheme. Lecture Notes in Economics and Mathematical Systems*, pp. 51–81. Springer, Berlin (2005)
- [30] Kall, P., Wallace, S.: *Stochastic Programming vol. 46*. John Wiley & Sons, Chichester (1994)
- [31] Luo, F., Dey, S., Mehrotra, S.: A cutting-plane and benders’ decomposition algorithm for two-stage distributionally robust convex programs. *Math. Program.*, 1–64 (2025)
- [32] Maggioni, F., Allevi, E., Bertocchi, M.: Bounds in multistage linear stochastic programming. *J. Optim. Theory Appl.* **163**, 200–229 (2014)
- [33] Maggioni, F., Allevi, E., Bertocchi, M.: Monotonic bounds in multistage mixed-integer stochastic programming. *Comput. Manag. Sci.* **13**(3), 423–457 (2016)
- [34] Maggioni, F., Cagnolari, M., Bertazzi, L., Wallace, S.W.: *Stochastic optimization*

- models for a bike-sharing problem with transshipment. *Eur. J. Oper. Res.* **276**(1), 272–283 (2019)
- [35] Maggioni, F., Cavagnini, R., Faccini, D.: Optimization-driven monotonic bounds for stochastic programs with applications in finance and operations management. In preparation (2026)
- [36] Mauttone, A., Cancela, H., Urquhart, M.E.: In: Crainic, T.G., Gendreau, M., Gendron, B. (eds.) *Public Transportation*, pp. 539–565. Springer, Cham (2021)
- [37] Melo, M.T., Nickel, S., Saldanha-da-Gama, F.: Facility location and supply chain management – a review. *Eur. J. Oper. Res.* **196**(2), 401–412 (2009)
- [38] Maggioni, F., Pflug, G.C.: Bounds and approximations for multistage stochastic programs. *SIAM J. Optim.* **26**(1), 831–855 (2016)
- [39] Maggioni, F., Pflug, G.C.: Guaranteed bounds for general nondiscrete multistage risk-averse stochastic optimization programs. *SIAM J. Optim.* **29**(1), 454–483 (2019)
- [40] Maggioni, F., Romeijnnders, W., Spinelli, A.: Lower bounds for two-stage stochastic programming problems with decision-dependent uncertainties. In preparation (2026)
- [41] Narum, B.S., Maggioni, F., Wallace, S.W.: On the safe side of stochastic programming: bounds and approximations. *Int. Tran. Oper. Res.* **30**(6), 3201–3237 (2023)
- [42] Rahmaniani, R., Crainic, T.G., Gendreau, M., Rei, W.: The benders decomposition algorithm: A literature review. *Eur. J. Oper. Res.* **259**(3), 801–817 (2017)
- [43] Rahmaniani, R., Crainic, T.G., Gendreau, M., Rei, W.: Accelerating the benders decomposition method: Application to stochastic network design problems. *SIAM J. Optim.* **28**(1), 875–903 (2018)
- [44] Rei, W., Cordeau, J.-F., Gendreau, M., Soriano, P.: Accelerating benders decomposition by local branching. *INFORMS J. Comput.* **21**(2), 333–345 (2009)
- [45] Roland, M., Forel, A., Vidal, T.: Adaptive partitioning for chance-constrained problems with finite support. *SIAM J. Optim.* **35**(1), 476–505 (2025)
- [46] Ramírez-Pico, C., Ljubić, I., Moreno, E.: Benders adaptive-cuts method for two-stage stochastic programs. *Transp. Sci.* **57**(5), 1252–1275 (2023)
- [47] Ramírez-Pico, C., Moreno, E.: Generalized adaptive partition-based method for two-stage stochastic linear programs with fixed recourse. *Math. Program.* **196**(1), 755–774 (2022)

- [48] Rockafellar, R.T., Uryasev, S.: Optimization of conditional value-at-risk. *J. Risk* **2**, 21–42 (2000)
- [49] Ruszczyński, A.: Decomposition methods in stochastic programming. *Math. Program.* **79**, 333–353 (1997)
- [50] Spinelli, A., Bezzi, D., Jabali, O., Maggioni, F.: A stochastic electric vehicle routing problem under uncertain energy consumption. *Transp. Res. Part C Emerging Technol.* **183**, 105480 (2026)
- [51] Schultz, R.: In: Infanger, G. (ed.) *Risk Aversion in Two-Stage Stochastic Integer Programming*, pp. 165–187. Springer, New York, NY (2011)
- [52] Shapiro, A.: Analysis of stochastic dual dynamic programming method. *Eur. J. Oper. Res.* **209**(1), 63–72 (2011)
- [53] Seo, K., Joung, S., Lee, C., Park, S.: A closest benders cut selection scheme for accelerating the benders decomposition algorithm. *INFORMS J. Comput.* **34**(5), 2804–2827 (2022)
- [54] Song, Y., Luedtke, J.: An adaptive partition-based approach for solving two-stage stochastic programs with fixed recourse. *SIAM J. Optim.* **25**(3), 1344–1367 (2015)
- [55] Spinelli, A., Maggioni, F., Ramos, T.R.P., Barbosa-Póvoa, A.P., Vigo, D.: A rolling horizon heuristic approach for a multi-stage stochastic waste collection problem. *Eur. J. Oper. Res.* **323**(1), 276–296 (2025)
- [56] Trukhanov, S., Ntaimo, L., Schaefer, A.: Adaptive multicut aggregation for two-stage stochastic linear programs with recourse. *Eur. J. Oper. Res.* **206**(2), 395–406 (2010)
- [57] Van Slyke, R.M., Wets, R.J.-B.: L-shaped linear programs with applications to optimal control and stochastic programming. *SIAM J. Appl. Math.* **17**, 638–663 (1969)
- [58] Wu, T., Zhang, J., Zhang, C., Liang, Z., Zhang, X.: Benders decomposition for stochastic facility location and production planning. *Comput. Oper. Res.* **186**, 107316 (2026)
- [59] Yuan, Y., Sen, S.: Enhanced cut generation methods for decomposition-based branch and cut for two-stage stochastic mixed-integer programs. *INFORMS J. Comput.* **21**(3), 480–487 (2009)